DMI
Ministry of Transport and Energy

Scientific Report 07-03

Overview and Application of Obstacle Resolved Models for Air Flow and Pollution Transport Simulations

Roman Nuterman

and

Alexander Baklanov

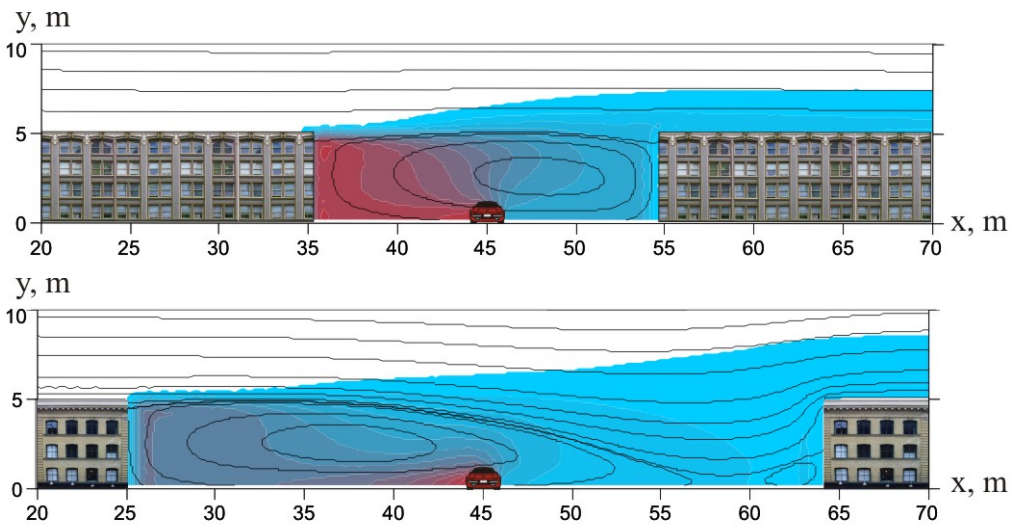

Copenhagen 2007

Colophon

Serial title:
Scientific Report 07-03

Title:
Overview and Application of Obstacle Resolved Models for Air Flow and Pollution Transport Simulations

Subtitle:
Urban Air Flow and Pollution CFD modelling

Author(s):
Roman Nuterman and Alexander Baklanov
Tomsk State University (TSU), Russia, nutrik@math.tsu.ru; DMI, Denmark, alb@dmi.dk

Other contributors:

Responsible institution:
Danish Meteorological Institute

Language:
English

Keywords:
Computer fluid dynamics (CFD) models, model down-scaling, micro-meteorology, urban air pollution, wind flows in complex terrain

Url:
www.dmi.dk/dmi/sr07-03

Digital ISBN:
978-87-7478-549-1

ISSN:
1399-1949

Version:
January 2007

Website:
www.dmi.dk

Table of Content:

Abstract

An overview of micro-scale meteorological models and turbulence closures for environmental flow modelling is presented. Advantages and disadvantages of different types of turbulence models for urban conditions are analyzed. As the first stage of developing tree-dimensional non-steady micro-scale model of atmosphere aerodynamics and pollution transport in urban canopy, two-dimensional version of the model is suggested, tested and validated versus wind-tunnel experiments. Strategy for further model improvements, including the downscaling/integration of the obstacle-resolved micro-scale model with a city-scale model, such as DMI-Enviro-HIRLAM, using the nesting technology is discussed.

1. Urban Air Flow and Pollution Transport Modelling

1.1. Introduction into the Problem

Recently, the atmosphere air quality decreasing has become one of the main reasons of people's health worsening in urban areas. The elements of urban canopy are the artificial obstacles for air flow, creating conditions for formation of stagnation regions, where the pollution from traffic and industry enterprises accumulates (*Oke, 1988*). Furthermore, the critical concentrations of pollution can be formed by an accident on the enterprises or act of terrorism and also by some atmospheric conditions above the urban areas. That is why the problem of highly polluted areas detection and studies of their formation conditions in cities arises.

Ambient air quality monitoring is an expansive problem and large cities may have only a few monitoring stations. If a location is not being monitored, than how the air pollution control authorities can determine the emission rate from a specific source required to valid ambient air quality standards? The answer to this question is to use the air quality models (mesoscale, city scale, obstacle resolved models) both to study the exchange between the source emissions and the resulting atmospheric pollutant concentrations, and also to provide a spatial and temporal interpolation of monitored data.

The emergence of increasingly powerful computers enabled the development of more powerful tools that have the potential to meet the new demand for predictions from models. These new tools are micro-scale meteorological models of prognostic or diagnostic type. Prognostic models are based on the Reynolds-Averaged Navier-Stokes (RANS) equations, whereas diagnostic models are less sophisticated and only ensure the conservation of mass. These two model types are presently supplemented by even simpler engineering tools. However, it is to be expected, that the latter will sooner or later be replaced by RANS codes or the even more complex Large Eddy Simulation (LES) models. The RANS codes belong to the family of Computational Fluid Dynamics (CFD) tools since they are used in various engineering problems. Micro-scale meteorological models are special because they are tailored to the needs of meteorologists. They are adjusted to domain sizes of the order of several decameters to a few kilometers (street canyons, city quarters). They usually use boundary conditions based on surface characteristics like land use, roughness and displacement thickness and they may contain modules that have the potential to simulate chemical transformations, aerosol formation or other important atmospheric physical-chemical processes.

In general CFD models show a good applicability for risk assessment in urban areas; however, their results can differ depending on turbulent closure models and some assumptions. For practical applications these models contain a substantial amount of empirical knowledge, not only in the turbulent schemes but also in the use of wall functions and in other parameterization schemes. It was shown by systematic studies, that the application of the same model by different modelers to the given problem (*Hall, 1997*) and application of different models by either the same or different modelers to the same problem (*Ketzel et al., 2001*) revealed significant differences. Nevertheless, these models are used in the preparation of decision with profound economic and political consequences. That is why the main objective of the COST Action 732 (http://www.mi.uni-hamburg.de/Home.484.0.html) is to improve and assure the quality of micro-scale meteorological models that are applied for flow predicting and transport processes in urban or industrial environments.

A structured model evaluation procedure is composed of many parts. These include model verification, i.e. assessments on whether the scientific foundation of the model is adequate for the purpose, and whether the computer code is producing output in accordance with the model specifications. Model validation is of similar importance, i.e. the comparison of model outputs with observed data. Model validation is not at all an easy task when undertaken in an objective and meaningful way. Data sampled within the urban canopy exhibit a large inherent variability, whereas micro-scale models are usually run with constant boundary conditions and produce steady-state results. Therefore, special emphasis must be given to the problem of what is really compared with each other. It can be shown that data from many short-term urban dispersion experiments have the character of snapshots that lack representativeness. Measurements carried out under identical conditions would not lead to identical results. Only the averaging over large ensembles of measurements taken under similar weather conditions provides mean values and standard deviations that are statistically meaningful.

The uncertainty resulting from systematic differences between numerical model simulations and data from the real world can also be quantified by repeating the field measurements under controlled conditions in a boundary layer wind tunnel (*Schatzmann and Leitl, 2002*). All major urban measurement campaigns that were carried out recently (DAPPLE, UK; BUBBLE, Switzerland; VALIUM, Germany, CAPITOUL, France; and the Joint Urban 2003 Tracer Experiment, USA) had a substantial wind tunnel component. Here, the field experiments were repeated under carefully controlled inflow and boundary conditions in order to investigate the uncertainty contained in the field data and, when it is necessary, to complete the data by measuring the missing quantities. This new experimental strategy which combines the advantages of both field and laboratory experiments is, in particular, useful for the micro-scale and provides unique opportunities. Additional experimental effort will be devoted to the generation of laboratory data that supports the development and/or justification of parameterizations used in micro-scale meteorological models.

The communication between meteorological and air pollution models is a problem which importance is often underestimated in the construction of air quality forecasting systems. The development programs are usually focused on the scientific and technical improvement of atmospheric flow and pollutant dispersion models, while comparatively little attention is devoted to the interfacing of different models. This condition often limits the possibility of dispersion models to access all the information that can be provided by new generation mesoscale meteorological models and it does not allow properly exploiting the scientific achievements in the description of the urban boundary layer (UBL) and urban scale circulations.

Often simple interface modules only take into account some averaged variables (e.g. wind, temperature and humidity) estimated by meteorological model simulations, while turbulence scaling parameters, atmospheric stability, dispersion coefficients and mixing height are diagnostically estimated by the interface itself. This kind of procedure is sometimes oversimplified and intrinsically cannot guarantee physical consistency of the different meteorological fields that describe the dynamic and thermodynamic status of the atmosphere.

On the other hand, Numerical Weather Prediction (NWP) models cannot provide all the physical variables that are needed by Urban Air Quality (UAQ) models or some of the meteorological fields are estimated by parameterizations and algorithms, which are not compatible with the modeling methods implemented in dispersion models.

The Integrated Systems for Forecasting Urban Meteorology, Air Pollution and Population Exposure (FUMAPEX) project (*Baklanov, 2006*; web-site: http://fumapex.dmi.dk) defined the development of interfaces from NWP models to UAQ models as one of its major objectives. This task is one of

the most important to enable the construction of reliable Urban Air Quality Forecasting Systems (UAQIFS). The various tasks that can be covered by interface modules (like data interpolation, meteorological fields downscaling, boundary layer parameterizations, estimation of dispersion coefficients) are very important.

1.2. Scale Interaction and Model Downscaling

Atmospheric processes on the micro-meteorological scale depend not only on the local features, but also on larger scale processes, e.g. those of the meso-meteorological or even regional scales.
Micro-meteorological and dispersion models for inhomogeneous areas, like urban domains, are sensitive to the choice of boundary conditions. In many research models and test studies the boundary conditions are simplified or artificial, mostly based on the assumptions of horizontal homogeneities in corresponding directions on the inlet and outlet boundaries of the considered domain.

However, in most of urban simulations for real conditions only a small part of the urban area is considered in a micro-meteorological model and urban heterogeneities outside the simulation domain affect the micro-scale processes. Therefore, it is important to build a chain of models of different scales with nesting of high resolution models into larger scale lower resolution models.

Different requirements should be considered for the main key parameters and levels of parameterisations for urban models of different scales (see Table 1). Usually, the micro-scale (street canyon) models are obstacle resolved and consider detailed geometry of the buildings and urban canopy, whereas the up-scaled city-scale (sub-meso) or meso-scale models consider parameterisations of urban effects or statistical descriptions of the urban building geometry.

Table 1: Key parameters for urban models of different scales (*COST715, 2003*)

Mesoscale models	Sub-meso scale models	Street canyon scale models
z_0, z_{0T}	$z_0(x)$, d(x)	
h_{UBL}	L_c, L_a, z_*	Detailed geometry
'Surface' fluxes (effective)	u_*^{IS}, H^{IS}, general: x_*^{IS}	$\bar{u}(h)$ second velocity scale for **horizontal** transport
Anthropogenic heat flux (non-surface) at some representative height	Dispersive fluxes	Heat exchange at vertical and horizontal building surfaces
Profiles of turbulent fluxes	Profiles of turbulent fluxes	Characteristic velocity variance in street canyon
Higher order moments?	Higher order moments (skewness, ...)	Higher order moments?
Synoptic forcing, average albedo	Mesoscale stability, albedo(x)	

One example of such model downscaling for urban meteorology and air pollution modelling, based on the FUMAPEX methodology (*Baklanov et al., 2002, 2006*), is demonstrated in Figure 1. This way can include downscaling from regional (or global) meteorological models to the urban-scale meso-meteorological models with statistically parameterised building effects and further downscaling to micro-scale obstacle-resolved CFD-type models.

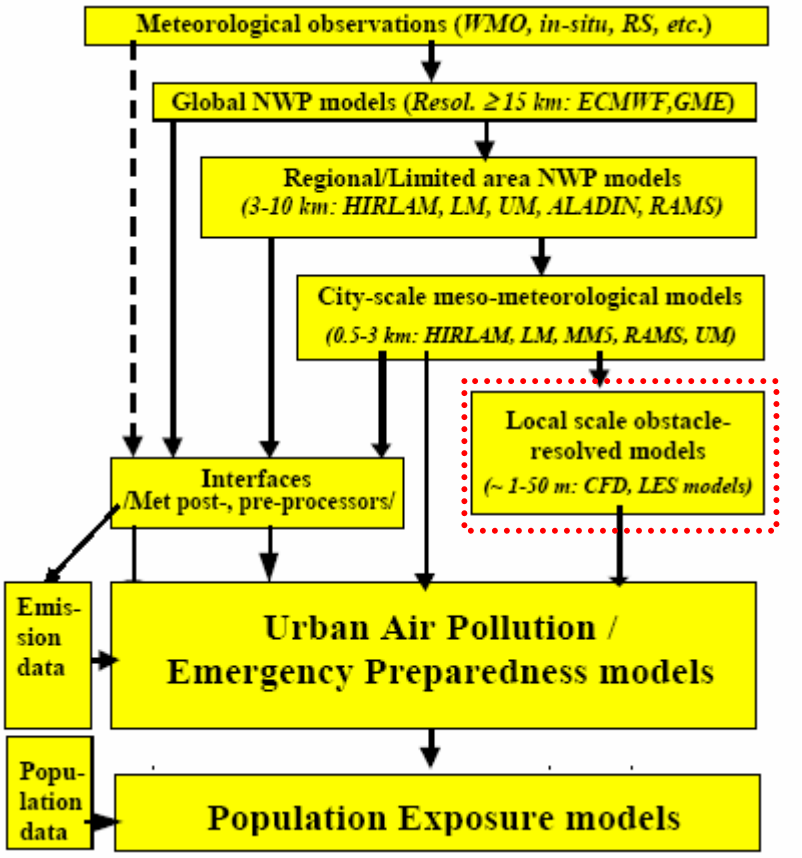

Figure 1. Structure for urban meteorology and air pollution modelling (within FUMAPEX UAQIFSs) by downscaling from the adequate meteorological or numerical weather prediction (NWP) models to the urban/micro-scale obstacle-resolved CFD type models.

In general sense, the scale interaction can play an important role in both directions: i.e. not only from a larger scale to the smaller micro-scale, but also from the urban/micro-scale to larger scale processes (e.g. atmospheric transport of harmful pollutants, initially released and dispersed in a street canyon; urban climate and wind climatology, etc.).

Therefore, two main types of the nesting techniques for the model downscaling can be chosen:
(i) one-way nesting, when effects of the local/micro-scale on the larger scale are not considered, and
(ii) two-way nesting, when the scale effects in both directions (from the meso-scale on the micro-scale and from the micro-scale on the meso-scale) are considered.
The second way is not always reasonable to consider, because the two-way nesting approach is more expensive in comparison with the one-way nesting. Therefore, for the considered specific problems it is recommended to do in advance (before suggesting the modelling system for end-users) a sensitivity study of the possible feedbacks from the micro-scale to larger scale processes.

One of the most important aspects in the model nesting is the necessary scale ratio (between the grid resolutions of the main and the nested models) to keep the suitable approximation and accuracy of the models. Long-term experience of many modellers shows that the ratio should not be higher than 3. Other important issue is the selection of the boundary and initial conditions for the nested model.

2. Overview of urban obstacle-resolved models

The environmental airflows, and flows in urban canopy are usually turbulent (*Colman, 1984*). The value of turbulence affects aerodynamics and pollution dispersion in urban street canyon (*Oke, 1988*). Air quality models are used to predict the transport and the turbulent dispersion of gases or aerosols after they are released into the atmosphere. Because of advances in computer speed and storage capabilities, now it is practical to apply CFD models to some of these air quality modeling scenarios involving short-range dispersion. The CFD models solves the basic time dependent Navier-Stokes equations, but using a small grid size (of order 1 m or even less). CFD models are especially useful when the plume is dispersing within arrays of obstacles such as building in urban or industrial areas, which also can have many pipe racks, tanks and other types of obstacles. Some CFD models are being run for specific urban building domains with links to urban neighborhood models and further links to mesoscale meteorological models (e. g., *Brown et al., 2000*).

2.1. Averaging approaches and turbulent closure models

Turbulent flow fields can be calculated with the Navier-Stokes system of equations averaged over space or/and time. When this averaging is performed, the equations describing the mean flow field contain the averages of products of fluctuating velocities. In general, this will result in more unknowns than the number of equations available. Such difficulty can be resolved by turbulence modeling with additional equations being provided to match the number of unknowns. Such models are designed to approximate the physical behavior of turbulence. There are numerous ways of averaging flow variables: time averaging, ensemble averaging, spatial averaging, and mass averaging (see Annex A).

2.2. System of time averaged (volume averaged) equations

The time-averaged equations for incompressible flows are given as the following:

Continuity:

$$\frac{\partial \overline{v}_i}{\partial x_i} = 0 .$$

Momentum:

$$\rho \frac{\partial \overline{v}_j}{\partial t} + \rho \overline{v}_i \frac{\partial \overline{v}_j}{\partial x_i} = -\frac{\partial p}{\partial x_j} + \frac{\partial}{\partial x_i}\left(\overline{\tau}_{ij} + \tau^*_{ij}\right), \tag{2.1}$$

where $\overline{\tau}_{ij} = 2\mu \overline{S}_{ij}$, $\overline{S}_{ij} = \frac{1}{2}\left(\frac{\partial \overline{v}_i}{\partial x_j} + \frac{\partial \overline{v}_j}{\partial x_i}\right)$, $\tau^*_{ij} = -\overline{\rho v_i' v_j'}$, $i = 1,2,3$,

v_i - projection of velocity vector on coordinate axis,
x_i - coordinate axis,
ρ - density,
t - time,
p - pressure,
μ - kinematic viscosity,
$\overline{\tau}_{ij}$ - stress tensor,
τ^*_{ij} - tensor of Reynolds stresses,
$\overline{S}_{ij}$ - strain rate tensor.

Energy (concentration):

$$\frac{\partial \overline{\Phi}}{\partial t} + \overline{v}_i \frac{\partial \overline{\Phi}}{\partial x_i} = -\frac{\partial}{\partial x_i}\left(\overline{q}_i - q_i^*\right), \tag{2.2}$$

where $\overline{q}_i = -\alpha \frac{\partial \overline{\Phi}}{\partial x_i}$, $q_i^* = -\overline{v_i' \Phi'}$, $i = 1,2,3$,

where α - diffusion factor of value $\overline{\Phi}$, and $\overline{\Phi}$ is average energy or concentration.

For time averaged incompressible flows, $-\overline{\rho v_i' v_j'}$ and $-\overline{v_i' \Phi'}$ are identified as the Reynolds (turbulent) stress and Reynolds (turbulent) heat (concentration) flux, respectively. These tensors and fluxes are extra unknowns. Thus, it is needed to add some equations; so, that the number of unknowns will be equal to the number of equations. This procedure is called the turbulent closure or modeling of turbulence.

2.3. Models of turbulence for RANS approach

A turbulence model is a computational procedure to close the system of mean flow Eqs. (2.1) and (2.2) so, that a more or less wide variety of flow problems can be solved. For most engineering purposes it is unnecessary to resolve details of the turbulent fluctuations. Only the effects of the turbulence on the mean flow are usually sought. In particular, we always need expressions for the Reynolds stresses in Eqs. (2.1) and the turbulent scalar transport terms in Eq. (2.2). A turbulence model for a general purpose CFD code is usually requested meeting the following requirements: a wide applicability, be accurate, simple and computationally economical. The most common turbulence models are classified: zero equation model – mixing length model, one-equation model, two-equation model, Reynolds stress equation model, algebraic stress model.

2.3.1. Two-equation models

From the classical models the mixing length and two-equation models are presently by far the most widely used and validated. They are based on the presumption that there exists an analogy between the action of viscous and Reynolds stresses on the mean flow and hypothesis of Kolmogorov-Prandtl about local isotropy. Both stresses appear on the right-hand-side of the momentum equation and in Newton's law of viscosity the viscous stresses are taken to be proportional to the rate of deformation of fluid elements.

There are many two-equation models for engineering and environmental flows are used in practice today. Among them is the k-ε model, which has been used most frequently for low-speed incompressible flows in isotropic turbulence. In this model, the turbulent stress tensor is given

$$\tau_{ij}^* = 2\mu_T \overline{S}_{ij} - \frac{2}{3}\rho k \delta_{ij},$$

where the turbulent (eddy) viscosity μ_T is defined as

$$\mu_T = \rho c_\mu \frac{k^2}{\varepsilon},$$

with $\varepsilon = \nu \overline{\frac{\partial v_i'}{\partial x_j} \frac{\partial v_i'}{\partial x_j}}$ being the turbulent kinetic energy k dissipation rate.

Thus, the turbulent viscosity contains two unknown variables, k and ε. It is, therefore, necessary that transport equations for k and ε are provided, which can be derived from the momentum equations. To avoid such additional unknowns, *Launder and Spalding* (*1972*) proposed the so-called k-ε model (see Annex A).

The basic idea of the k-ω model was originated by *Kolmogorov* (*1942*) with turbulence associated with vorticity, ω, being proportional to $k^{1/2}/l$,

$$\omega = c\frac{k^{1/2}}{l},$$

where c is a constant. Thus, the eddy viscosity may be written as

$$\mu_T = \rho k/\omega .$$

The transport equations for k and ω proposed by *Wilcox* (*1988*), (see Annex A).

The mathematical tool described above widely applies for computation of airflow in urban canopy. For instance, the two-dimensional non-steady Reynolds equation and k-ε model of turbulence are used in study (*Huang et al., 2000*) for determination of turbulent structure of flow. However, some atmospheric boundary layer (ABL) features and effects cannot be described by the standard two-equation models, because their constants were estimated mostly for engineering flow problems. Therefore, modifications of some constants in such models are required for correct prediction e.g. in stable stratified ABLs, see *Baklanov* (*2000*).

Recently the group of European scientists, working at TRAPOS project, has created models such as CHENSI-1, CHENSI-2, MIMO, MISKAM, TASCflow, for calculation of pollution from traffic (*Louka et al., 2001*). The basic system of equations in these models includes non-steady Reynolds equations for modeling of averaged turbulent motions. For turbulence closure k-ε and k-ω models of turbulence are used. These models can be applied for prediction of pollution transport in street canyon and also in urban blocks.

2.3.2. Reynolds stress models

Effects of streamline curvature, sudden changes in strain rate, secondary motion, etc. can not be predicted in the two-equation models. The second order closure models or Reynold stress models are designed to handle these features. The Reynolds stress transport equation has the following form:

$$\frac{\partial \tau_{ij}^*}{\partial t} + \frac{\partial}{\partial x_k}\left(\bar{v}_k \tau_{ij}^*\right) = A_{ij} + B_{ij} + C_{ij} + D_{ij}, \tag{2.3}$$

where A_{ij}, B_{ij}, C_{ij}, and D_{ij} denote production, dissipation (destruction), diffusion, and pressure strain, respectively; and

$$A_{ij} = -\tau_{ik}^* \frac{\partial \bar{v}_j}{\partial x_k} - \tau_{jk}^* \frac{\partial \bar{v}_i}{\partial x_k},$$

$$B_{ij} = -2\mu \overline{\frac{\partial v_i'}{\partial x_k}\frac{\partial v_j'}{\partial x_k}},$$

$$C_{ij} = \frac{\partial}{\partial x_k}\left[-\left(\rho \overline{v_i' v_j' v_k'} + \overline{p' v_i'}\delta_{ik}\right) + \mu \frac{\partial \tau_{ij}^*}{\partial x_k}\right],$$

$$D_{ij} = \overline{p'\left(\frac{\partial v_i'}{\partial x_j} + \frac{\partial v_j'}{\partial x_i}\right)}.$$

Note, that new variables are introduced in C_{ij} and D_{ij}, whereas A_{ij}, B_{ij} do not contain new variables. Thus, we must simulate the diffusion transport and pressure-strain tensors. Although dissipation occurs at the smallest scales and one can use the Kolmogorov hypothesis of local isotropy, it may become anisotropic close to the wall, and thus, modeling is needed.

Dissipation rate tensor is represented as in k-ε model (*Launder and Spalding, 1972*). Diffusion tensor was modeled by *Launder et al.* (*1975*). The ratio for correlation of pressure fluctuation and strain rate were also proposed by *Launder et al.* (*1975*).

2.3.3. Algebraic Stress Model (ASM) and Non-Linear Eddy Viscosity Model (NLEVM)

The purpose of ASM is to avoid the solution of differential equations, and to obtain the Reynolds stress components directly from algebraic relationships. *Rodi* (*1976*) considered that advection-diffusion transfer of correlation $\overline{u_i' u_j'}$ is proportional to the kinetic energy k:

$$\frac{\partial \tau_{ij}^*}{\partial t} + \bar{v}_k \frac{\partial \tau_{ij}^*}{\partial x_k} - \frac{\partial}{\partial x_k}\left(\nu \frac{\partial \tau_{ij}^*}{\partial x_k} + \rho \overline{v_i' v_j' v_k'} + \overline{p' v_i'} \delta_{ik} \right) \approx$$

$$\frac{\tau_{ij}^*}{k}\left(\frac{\partial k}{\partial t} + \bar{v}_k \frac{\partial k}{\partial x_k} - \frac{\partial}{\partial x_k}\left[\nu \frac{\partial k}{\partial x_k} + \frac{\rho \overline{v_j' v_j' v_k'} + \overline{p' v_j'} \delta_{jk}}{2\rho} \right] \right).$$

This approximation leads to nonlinear algebraic equations, which can be used for determination of Reynolds stress tensor, that is

$$\frac{\tau_{ij}^*}{\rho k}\left(\tau_{mn} \frac{\partial \bar{v}_m}{\partial x_n} - \rho\varepsilon \right) = -\tau_{ik}^* \frac{\partial \bar{v}_j}{\partial x_k} - \tau_{jk}^* \frac{\partial \bar{v}_i}{\partial x_k} + \varepsilon_{ij} - \overline{p'\left(\frac{\partial v_i'}{\partial x_j} + \frac{\partial v_j'}{\partial x_i} \right)}. \qquad (2.4)$$

If we suggest that averaged strain rate vanishes to zero, then Eq. (2.4) is simplified to

$$\tau_{ij}^* = \frac{k}{\varepsilon}\left(D_{ij} + B_{ij} \right),$$

where $D_{ij} = c_1 \frac{\varepsilon}{k}\left(\tau_{ij}^* + \frac{2}{3}\rho k \delta_{ij} \right)$, $B_{ij} = -\frac{2}{3}\rho\varepsilon\delta_{ij}$, c_1 is a constant.

Thus, if averaged strain rate is zero, so we have

$$\tau_{ij}^* = -\frac{2}{3}\rho k \delta_{ij}.$$

This expression assumes, that algebraic model is constrained by the property isotropy of turbulence. Thus, the ASM for Reynolds stresses is not acceptable for prediction of sudden change of averaged strain rate. If the algebraic models are combined with k-ε model, then it is possible to find satisfactory results for secondary motions (*Dumuren, 1991*).

The application of algebraic ratios with two-equation models of turbulence leads to better results of aerodynamics modeling of urban canopy as it was displayed by *Nuterman and Starchenko* (*2005*). However, it is connected with a necessity of solving additional transfer equations, and also with problem of numerical stability at numerical solving of problem.

Now, stress-transport models of turbulence can offer a more reliable way of handling complex strain fields, but schemes of this type in a fairly widespread use have been developed with an idea that any rigid surface can (as far as the turbulence is concerned) be regarded as infinite and plane. That constraint is inapplicable to the great majority of flows in the mechanical engineering sector that might use CFD for their analysis. Quite apart from this serious deficiency, the stress transport schemes are still regarded as requiring too much computer resource for industrial use, especially in three-dimensional (3-D) flows where all stress components are non-zero.

An alternative, much simpler, route is available for approximating the Reynolds stresses which adopts non-linear algebraic connection between stress and strain. Such relationships may be found by simplifying stress-transport models (so-called algebraic stress models, ASMs). However, in view of the current limitations of such schemes above mentioned, it is best to regard them simply as conjectured generalizations of the eddy-viscosity approach, containing quadratic and, occasionally,

higher-order products of the strain and vorticity tensors. The earliest schemes go back to the 1970s (*Pope, 1975*), although, in the recent few years, there have been concerted efforts by many different groups world wide.

If we retain simply quadratic terms, the basic stress-strain relationship may be written as follows:

$$a_{ij} = \frac{\overline{v_i' v_j'} - \frac{2}{3}\delta_{ij}k}{k} = -\frac{\nu_t}{k}S_{ij} + c_1\frac{\nu_t}{\varepsilon}\left(S_{ik}S_{kj} - \frac{1}{3}S_{kl}S_{kl}\delta_{ij}\right) + c_2\frac{\nu_t}{\varepsilon}\left(\Omega_{ik}S_{kj} + \Omega_{jk}S_{ki}\right) + c_3\frac{\nu_t}{\varepsilon}\left(\Omega_{ik}\Omega_{jk} - \frac{1}{3}\Omega_{lk}\Omega_{lk}\delta_{ij}\right),$$

where:

$$S_{ij} = \left(\frac{\partial\overline{v}_i}{\partial x_j} + \frac{\partial\overline{v}_j}{\partial x_i}\right), \Omega_{ij} = \left(\frac{\partial\overline{v}_i}{\partial x_j} - \frac{\partial\overline{v}_j}{\partial x_i}\right) - \varepsilon_{ijk}\Omega_k$$

and Ω_k is the rotation rate of coordinate system. There are several schemes for empirical coefficients c_μ, c_1, c_2, c_3 (*Speziale, 1987*; *Nisizima and Yoshizawa 1987*; *Rubinstein and Barton 1990; Shih et al., 1993*). All of these studies showed very different values of coefficients, depending on what flow or flow features were chosen to predict. This seems to indicate that, at quadric level, only slightly greater generality is achievable than with the usual linear eddy-viscosity model. Such type of models was modified in study of *Craft et al.* (*1996*) by adding cubic stress-strain relation; the greater flexibility that this has brought enables stress levels to be captured over a far wide range of complex strain fields that hitherto.

At present time, there are some studies (*Ehrhard and Moussiopoulus, 2000*) for using of the NLEVM two-equation models of turbulence developed by *Craft et al.* (*1996*) and *Lien et al.* (1996) for calculation of flows in urban canopy. The use of such models allows increasing accuracy of airflow calculation and pollution transport, while increasing of computational time is about 15-20% in comparison with linear models eddy-viscosity (k-ε and k-ω). If NLEVM models compared with the differential models for turbulent stresses, in the point of precision of flow pattern prediction, then NLEVM formulation surrender. However, its realization needs less of computational costs (*Gatski and Jongen, 2000*). Furthermore, while using NLEVM approach it is difficult to take account the buoyancy as in Reynolds stress transport models.

2.4. Large Eddy Simulation

Despite a great deal of effort and advancement in turbulence modeling for the past century, difficulties still remain in geometrically and physically complicated flow fields. The large eddy simulation (LES) is an alternative approach toward achieving a goal of more efficient turbulent flow calculations. Here, by using more refined meshes than usually required for the RANS system of equations, the large eddies are calculated (resolved) whereas small eddies are modeled. The rigor of LES in terms of performance and ability is somewhere between RANS and the direct numerical simulation (DNS). There are two major steps involved in the LES analysis: filtering and subgrid scale modeling.

In order to define a velocity field containing only the large-scale components of the total field, it is necessary to filter the variables of the Navier-Stokes system of equations, resulting in the local average of the total field (see Annex B). To this end, using one-dimensional notation for simplicity, the filtered variable f may be written as

$$\bar{f} = \int G(x,\xi) f(\xi) d\xi ,$$

with $\int G(x,\xi) d\xi = 1$,

where $G(x,\xi)$ is the filter function which is large only when x and ξ are close together. Frequently, the Box, Gaussian and Fourier cutoff filters are usually applied (see Annex B).

The solution of the filtered Navier-Stokes system of equations enables only the large eddies to be resolved, leaving the small eddies still unresolved. Since these small eddies are more or less isotropic, the modeling is much easier than in the case of RANS. However, for compressible flows, particularly for supersonic and hypersonic flows in which turbulent heat flux, turbulent diffusion, and viscous diffusion may become significant, the subgrid scale (SGS) modeling process is far from satisfactory.

There are different approaches for developing the SGS turbulent stress models. The eddy viscosity model is most widely used in which the global effect of SGS terms is taken into account, neglecting the local energy events associated with convection and diffusion (*Smagorinsky*, *1963; Yoshzawa*, *1986*).

In such models, the traditional gradient-diffusion approach (molecular motion) is used; so, that the turbulent stress tensor for compressible flows is written as

$$\tau_{ij}^{*} = 2\mu_T \left(\bar{S}_{ij} - \frac{1}{3} \bar{S}_{kk} \delta_{ij} \right) - \frac{2}{3} \bar{k} \delta_{ij}$$

$$\mu_T = \bar{\rho} (C_s \Delta)^2 \left| \bar{S} \right|, \ \Delta \cong l, \ \bar{S}_{ij} = \frac{1}{2} \left(\frac{\partial \bar{v}_i}{\partial x_j} + \frac{\partial \bar{v}_j}{\partial x_i} \right), \ \left| \bar{S} \right| = \left(2 \bar{S}_{ij} \bar{S}_{ij} \right)^{1/2},$$

where C_s is the Smagorinsky constant, l is reference turbulent scale and $\bar{k}$ is the subgrid scale turbulent kinetic energy.
This constant can be evaluated by assuming the existence of an inertial range spectrum. To this end, it has been suggested by *Lilly* (*1966*) that $C_s \cong 0.18$.

It has been shown in the literature that superior results may be obtained by updating the model coefficients based on the current flow fields, known as the dynamic model (*Germano et al., 1991*). Here, in addition to the subgrid scale filtering, a test filter is introduced with the test filter width Δ_t larger than the grid filter width Δ (usually $\Delta_t = 2\Delta$ is used) in order to obtain information from the resolved flow field. Based on this model, *Lilly* (*1992*) suggested that

$$\mu_T = C_d \bar{\rho} \Delta^2 \left| \bar{S} \right|, \tag{2.5}$$

with

$$C_d = \frac{A_{ij} M_{ij}}{M_{km} M_{km}}, \ A_{ij} = \left\langle \overline{\rho v_i} \bar{v}_j \right\rangle - \frac{\left\langle \overline{\rho v_i} \right\rangle \left\langle \overline{\rho v_j} \right\rangle}{\left\langle \bar{\rho} \right\rangle},$$

$$M_{ij} = -2\Delta_t^2 \left\langle \bar{\rho} \right\rangle \left\langle \left| \bar{S} \right| \right\rangle \left\langle \bar{S}_{ij} - \frac{1}{3} \bar{S}_{kk} \delta_{ij} \right\rangle + 2\Delta^2 \left\langle \bar{\rho} \left| \bar{S} \right| \left(\bar{S}_{ij} - \frac{1}{3} \bar{S}_{kk} \delta_{ij} \right) \right\rangle,$$

where $\langle \ \rangle$ implies a test filtered quantity (see Annex B).

The advantages of dynamic models were shown in numerous investigations, e.g. (*Balaras et al., 1995; Jordan, 2001; Moin et al., 1991; Piomelli, 1993; Yang and Ferziger, 1993*).

Now, besides models based on RANS approach, actively applied models for calculation of flows in street canyons based on large eddy approach for instance in studies (*Walton et al., 2002*; *Chun-Ho*

et al., 2004) applied dynamic model.

The studies (*Cheng et al., 2003*; *Rodi, 1997*) show that the complex features (e.g., vortex shedding, large separation zones, topology of the reattachment lines bordering the recirculation regions, fine-scale flow structures near the side walls, etc.) of the fully developed flow within and above building-shaped structures are reproduced better with LES than RANS calculations, albeit at the disadvantage of much greater computational times.

Many CFD models, based on the RANS equations, use the standard k-ε turbulence models, which were originally developed for hydro-dynamical engineering problems. For example, for urban canyons this model with the linear stress-strain relation is violated in complex flow and has to be improved using non-linear two-equation turbulence models (*Ehrhard and Moussiopoulus, 2000*). LES models show a substantially better correspondence with measurement data in urban areas (e.g., *Walton et al., 2002*) and have good perspectives. But they are more expensive, and therefore, their usage is limited.

2.5. Pollution transport models

Turbulent diffusion of matter and heat is of primary importance in industrial, chemical and atmospheric studies. Since a source of such contaminants is in many cases close to solid boundaries, the study of diffusion in turbulent boundary layer flows is of special interest.

Applying the RANS we can derive the diffusion equation for a real shear flow for atmospheric problem. The transport equation for the contaminant concentration C is

$$\frac{\partial C}{\partial t} + v_i \frac{\partial C}{\partial x_i} = \frac{\partial}{\partial x_i}\left[D \frac{\partial C}{\partial x_i} - \overline{v_i' c'} \right] + S_p , \tag{2.6}$$

where D is the molecular diffusion coefficient and S_p is the source term. For deriving the closed form of pollution transport equation the turbulent contaminant flux vector $\overline{v_i' c'}$ needs to be defined.

To describe an evolution of the concentration field of a plume emitted from a ground line source in urban canopy, the k-ε model is usually applied. Often, Eq. (2.6) is closed with the help of the down-gradient k model:

$$-\overline{v_i' c'} = D_T \frac{\partial C}{\partial x_i} . \tag{2.7}$$

It is able to reproduce structural features of the concentration field transformation because the turbulent diffusion coefficient D_T obtained from parameters k and ε varies not only with the thickness of the boundary layer, but also with the distance from the source. The k-ε turbulence model is a non-local theory with respect to k, ε and these parameters are determined by history.

The Eulerian diffusion model includes equations for the mean velocity, the turbulence kinetic energy k, the dissipation ε and the mean concentration of matter. An algebraic model for the turbulent mass-flux vector $\overline{v_i' c}$ derived from the closed differential transport equation for this correlation using the assumption of equilibrium turbulence (*Launder, 1978*). This approximation can be written, assuming the linear Boussinesq hypothesis for the Reynolds stress tensor $\overline{v_i' v_j'}$, as the explicit algebraic mass-flux model (*Kurbatskii and Yakovenko, 2000*):

$$-\overline{v_i' c'} = D_T \frac{\partial C}{\partial x_i} - \frac{1}{C_{1c}} \frac{k}{\varepsilon} \left\{ \left[2\nu_T + (1 - C_{2C}) D_T \right] S_{ik} + (1 - C_{2C}) D_T \Omega_{ik} \right\} \frac{\partial C}{\partial x_k} , \tag{2.8}$$

where $S_{ik} = \frac{1}{2}\left(\frac{\partial \overline{v}_i}{\partial x_k} + \frac{\partial \overline{v}_k}{\partial x_i}\right)$, $\Omega_{ik} = \frac{1}{2}\left(\frac{\partial \overline{v}_i}{\partial x_k} - \frac{\partial \overline{v}_k}{\partial x_i}\right)$, $D_T = \frac{\nu_T}{Sc_T}$, $\nu_T = \frac{C_\mu f_\mu k^2}{\varepsilon}$, Sc_T is the turbulent Schmidt number ($C_\mu = 0.09$, $C_{1C} = 3.0$, $C_{2C} = 0.4$). The damping near-wall function $f_\mu = \left(1 + 3.45/\sqrt{\mathrm{Re}_t}\right)\left[1 - \exp\left(-y^+/70\right)\right]$ ($y^+ = \rho u_\tau y/\mu$ - non-dimensional wall distance, u_τ - friction velocity, Re_t - turbulent Reynolds number) is introduced into the turbulent viscosity coefficient ν_T to allow direct integration of the model to a wall in order to satisfy the asymptotic behavior of the turbulence statistics in the near-wall region.

Using closure Eq. (2.7) or the fully explicit algebraic expression, Eq. (2.8), the closed form of Eq. (2.6) is obtained. Model (2.7), (2.8) can be used in conjunction with any two-equation or Reynolds-stress model for the velocity field, thus greatly simplifying a numerical solution of pollutant transfer problems. It could be easily extended to buoyant flows without having to solve additional equations.

For LES approach we apply the filter to the passive scalar transport equation, which yields the resolved scale transport equation:

$$\frac{\partial \overline{C}}{\partial t} + \frac{\partial \overline{v}_i \overline{C}}{\partial x_i} = -\frac{\partial q_i}{\partial x_i} + \frac{\partial}{\partial x_i}\left[D\frac{\partial \overline{C}}{\partial x_i}\right] + S_p ,$$

where $\overline{C}$ is the resolved-scale scalar, and D is the mass diffusivity. The first term on the right-hand side of equation represents turbulent diffusion whose subgrid-scale fluxes

$$q_i = \overline{v_i C} - \overline{v}_i \overline{C} ,$$

are smaller than the filter width and can be modeled by the eddy-diffusivity model

$$q_i = \frac{\nu_T}{Sc_T}\frac{\partial \overline{C}}{\partial x_i} .$$

Thus, the transport equation for concentration for LES approach is

$$\frac{\partial \overline{C}}{\partial t} + \overline{U}_i \frac{\partial \overline{C}}{\partial x_i} = \frac{\partial}{\partial x_i}\left[(D + D_T)\frac{\partial \overline{C}}{\partial x_i}\right] + S_p ,$$

where $D_T = \frac{\nu_T}{Sc_T}$ and ν_T is defined as by *Smagorinsky* (*1963*) or dynamically Eq. (2.5).

2.6. Heat transfer models

One of the main topics of interest, especially under conditions of low wind speed, is the influence of wall heating in street canyons due to solar radiation incident on one or more walls during the day. The influence of different buoyancy effects due to canyon wall heating has not previously been assessed through wind tunnel simulations under carefully controlled conditions, because it is a challenging problem to match the necessary similarity laws for velocity and temperature via an appropriate Froude number. The effect of wall heating on the flow and pollution dispersion characteristics within the canyon is likely to be the greatest when the windward-facing wall is heated. This is because the buoyancy forces generated at that wall by the heating directly oppose the downward inertial forces in the same region that are associated with the dominant canyon vortex. It is anticipated, from previous numerical predictions (*Mestayer et al., 1995*), that, under certain conditions, the buoyancy forces will be large enough to disrupt the canyon vortex to form a different regime with consequent effects on the local flow and pollutant dispersion characteristics.

To take into account of buoyancy ρg is added to vertical component of velocity, where ρ - density is a function of temperature for incompressible turbulent inert flow (Boussinesq approximation).

When solar radiation heats the building walls or ground, the air density changes due to increasing of air temperature. The rate change in the air density due to an increase in temperature is estimated by:

$$\left(\frac{\rho-\rho_n}{\rho_n}\right)=-\beta(\theta-\theta_n),$$

where β is the thermal expansion coefficient, ρ_n and θ_n are the reference density and temperature. If we consider two-parameter model of turbulence the source terms which will provide the buoyancy effect in k and ε equations are $-\beta g_j\overline{u_j'\theta'}$ and $-\beta g_j\overline{u_j'\theta'}\frac{\varepsilon}{k}$, respectively.

For description of stresses $\overline{u_j'\theta'}$ transfer the additional transport Eq. (2.2) is required. The similar approach applies for LES modeling for heat transfer problem.

2.7. Parameterization of traffic induced turbulence and urban vegetation

Moving vehicles intensify both micro- and large scale mixing processes in the environment by inducing turbulence and enhancing advection by entraining masses of air in the direction of vehicle motion.

Dispersion of pollutants, originating from the traffic, is usually a rather short distance process, and it is obvious that the actual geometry of the adjacent area plays an important role. The canopy layer is strongly disturbed by buildings and other obstacles in urban areas, which may influence the local concentrations by more than one order of magnitude. Accurate mathematical description of vehicles behavior and geometry of calculated domain serves as a basic for prediction of air pollution field in the pedestrian area.

There are several approaches of solving the problem of traffic motion prediction in urban air quality models. The study (*Katolicky and Jicha, 2005*) presents a car motion approach based on CFD calculations using an Eulerian approach to the continuous phase (air) and a Lagrangian approach to the discrete phase of moving objects (vehicles) in different situations in cities to predict pollutants dispersion from traffic. This parameterization includes necessity to add the source term in momentum equations to describe the drag force of air and term in k equation to predict the production of kinetic energy by vehicles.

Other authors (e.g. *Baumer et al., 2005*) described such effects through specific coefficients of diffusion in equations of concentration and kinetic energy transfer and also by source terms. Moreover, this study includes the sedimentation process for emitted particles, described by advection-diffusion equation for mass density of particles. The velocity of deposition is obtained by balancing gravitational force and Stoke's frictional force assuming spherical particles.

The modeling of air flow and scalar transport within urban vegetation is very difficult problem due to the complex turbulent structure in these elements of urban canopy. This areas defined by very big dissipation of turbulent energy due to formation of small dissipative eddies. Usually, to solve this problem the two-equation turbulence models for RANS approach are applied. The descriptions of processes in urban vegetation are implemented by source terms in momentum equations and in the equations of turbulence model (*Kimura et al., 2003*). Such approach gives a satisfactory agreement with experimental data. However, some authors introduce the second and the third order closure schemes for vegetation canopy as (*Katul and Albertson, 1998*). The use of these models results in more realistic prediction of air flow, but has the disadvantage of a greater computational times because of increased system of equations for Reynolds stresses and triple-velocity correlation.

Also the similar approach applied for LES modeling. Commonly, for this method of turbulence modeling for describing of air flows in urban vegetation the averaged momentum equations and *k* model of turbulence with source terms in their right hand side are used (*Dwyer et al., 1997*).

2.8. Boundary conditions

The problem of mathematical simulation of turbulent flows near walls appears in many practical applications. It is well known that turbulence vanishes near a wall due to the no-slip boundary condition for the velocity as well as the blocking effect caused by the wall. In vicinity of the wall, there is a thin sublayer with predominantly molecular diffusion and viscous dissipation. The sublayer has a substantial influence upon the remaining part of the flow. An adequate numerical model resolution in the sublayer requires a very fine mesh because of the thinness of the sublayer and high gradients of the solution. It makes a model used time consuming and often not suitable for engineering applications. Because of the low turbulent Reynolds number in the sublayer, models that resolve the sublayer are called the low-Reynolds-number (LR) models.

So-called the high-Reynolds-number (HR) models do not provide resolution of the viscous sublayer. In this type of models the sublayer domain is not directly resolved. It significantly saves computational efforts. In the HR models, the boundary conditions or near-wall profiles are represented by wall functions.

Often the inflow boundary conditions for RANS approach for micro scale models are dependent of the inflow information or ideal inflow profile. Usually, the outflow boundary conditions of such models are zero normal first derivative for all flow parameters and pressure correction to ensure overall mass conservation. Zero normal first or second derivatives or boundary layer condition are used on the top of the domain. In the near wall region the logarithmic law of the wall for velocity and turbulence values and zero normal first derivative, or zero normal second derivative for conservation are used.

At high Reynolds numbers, the LES cannot resolve the eddies in the semi-viscous near-wall region, unless a very fine mesh is used. Even if such a fine mesh could be accommodated normal to the wall, the reduction in the turbulent scale in all three directions implies the need for similar refinements in the other two directions. This is not tenable on economic grounds and necessitates the adoption of an approximate treatment which bridges the near-wall layer.

Alternative approaches are based on the use of conventional low-Re turbulence models or semi-analytical ‘‘wall laws’’. For example, in study (*Walton et al., 2002*) first, the friction velocity is calculated:

$$U_\tau = \sqrt{\frac{U_\parallel \nu}{y_w}} \quad \text{if } U_\parallel \le \frac{y_0^+ \nu}{y_w}, \tag{2.9}$$

or

$$U_\tau = \frac{U_\parallel}{(1/\kappa)\ln(y_w U_\tau / \nu) + 5.5} \quad \text{if } U_\parallel > \frac{y_0^+ \nu}{y_w}, \tag{2.10}$$

where $y_0^+ = 11.6$ is the thickness of the viscous sublayer in dimensionless wall units. $U_\parallel$ denotes the component of the fluid velocity parallel to the wall at the first active grid cell, and y_w is the distance of this node from the wall. κ is von Karman’s constant ($\kappa = 0.4$). Thus, the no-slip condition, Eq. (2.9), is used when the first grid cell lies within the viscous sublayer, otherwise the log law of the wall, Eq. (2.10), is used. Having obtained the friction velocity, the local wall shear stress is calculated from

$$\tau_w = \rho u_\tau^2 .$$

Automatic switching between no-slip and approximate wall functions is convenient since anticipating the thickness of the viscous sublayer is not trivial when dealing with complex flows. Eqs. (2.9) and (2.10) are solved for all wall grid cells. Effectively, it is assumed that the local flow is everywhere fully developed.

3. Model verification strategy and urban experimental datasets

In order to predict the dispersion of harmful materials released in or near an urban environment, it is important to first understand the complex flow patterns which result from the interaction of the wind with buildings and, more commonly, clusters of buildings. Recent advances in the application of CFD models to such problems have show a great promise, but there is need for high-quality data with which to evaluate CFD models.
Several types of experimental data can be used for this purpose, including:

(i) Measurement campaigns in urban areas,
(ii) Wind tunnel studies,
(iii) High resolution LES or DNS experiment datasets.

Measurements in urban street canyons are ideal for model validation because they present real system observations, however, the measurement conditions (meteorological, first of all) cannot be fixed, planned or perfectly forecasted and the measurement points are not numerous and far from each other. Detailed investigations of wind behavior measurements are carried out in real street canyons (*Chang et al., 2004; Neophytou and Britter, 2004*). Basically, these investigations show the formation of vortex in urban street canyon, but this vortex is not usually developed especially due to slight velocity wind. Asymmetrical form of canyons, low velocity vector, traffic motion, are created velocity field far from ideal in street canyon. Moreover, the researchers discovered that the basic factor influenced on the pollution transfer pattern in street canyon is configuration of urban street canyon that is form.

The investigation of street canyon in wind tunnel is easier than observation in real scale; moreover the conditions of experiment can be governed. In studies (*Gerdes and Olivari, 2000; Brown et al., 2000*) have discovered that concentration of atmospheric pollutant, depending on skew ness of canyon's geometry and ratios of their geometrical proportions, decreases exponentially at vertical directions and increases at leeward side.

Nowadays, several urban datasets, which actively used for verification of mathematical models, such as BUBBLE, ESCOMPTE, DAPPLE, URBAN2000, CAPITOUL, etc., are available.

For instance, BUBBLE stands for 'Basel UrBan Boundary Layer Experiment' (*Rotach et al., 2004*) and was an effort to investigate in detail the boundary layer structure in a mid-sized European city, namely that of Basel, Switzerland. The philosophy of BUBBLE was to combine long-term (1-year) near-surface and remote sensing observations on the one hand with numerical and physical modeling on the other hand. It is felt that only a decent combination of the three approaches can lead to a substantial improvement of the knowledge in a highly complex environment as an urban boundary layer.

During an intensive observation phase (IOP) - towards the end of the full-scale observations - a substantial number of specialized projects were performed in the city of Basel taking advantage of the extraordinary dense existing network of meteorological observations. These included studies on

street canyon energetics and satellite ground-truth. The project that was linked closest to the overall goals of COST 715 consisted of a series of tracer release experiments with near roof releases (*Rotach et al., 2003*).

DAPPLE (Dispersion of Air Pollution & Penetration into the Local Environment) is a 4-year consortium research project funded by the UK EPSRC Engineering for Health, Infrastructure and Environment Programme (*Neophytou and Britter, 2004*). The project brings together multidisciplinary expertise from six universities capable of undertaking fieldwork, wind tunnel and computational simulations in order to provide a better understanding of the physical processes affecting street and neighbourhood scale flows of air, traffic and people, and their corresponding interactions with the dispersion of pollutants.

The fundamental understanding gained will be used in the evaluation and development of appropriate decision support tools and guidelines for their application. This will help lead towards sustainable development of safer, more pleasant cities. As far as possible, the DAPPLE deliverables are intended to be of generic value and applicable both within UK urban areas and others overseas.

The fieldwork is based at and around the Marylebone Road and Gloucester Place intersection in Central London. The street canyon intersection is of interest as it provides the basic case study to demonstrate most of the factors that are applicable in a wide range of urban topologies.

It is natural that experimental investigations cannot be always conducted for modeling different cases of geometry of street canyon and various scenario of pollution. Furthermore, errors can be arisen by inaccurate boundary conditions and reduced scales. Usually such experiments need for verification of mathematical models.

The ongoing COST Action 732: 'Quality Assurance and Improvement of Micro-Scale Meteorological Models' (http://www.mi.uni-hamburg.de/Home.484.0.html) is working now with elaboration of Recommendations for the quality assurance procedure for urban micro-scale wind-flow and dispersion models.

4. Formulation of micro-scale model for air flow and pollution transport in urban canopy

The authors of this report in different years realized several numerical micro-scale models for air flow and pollution transport in urban canopy. One of such problem-oriented CFD modeling systems was developed by *Baklanov* (1988, 2000) and *Amosov and Baklanov* (1992). It included the following assumptions, possibilities, and applications:

- 3D compressible or incompressible air flow and air pollution dynamics,
- Complex geometry by the method of fiction domains or terrain-following σ-coordinates,
- Sub-grid turbulence closure, modified k-ε, k-l models,
- Radiation and thermal budget of arbitrary oriented surface,
- Artificial and ventilation sources of air dynamics and circulation,
- Urban/industrial air flows and pollution problems,
- Indoor air dynamics and ventilation,
- Microclimate and pollution mountain valleys and circuses,
- Mining ventilation and microclimate of open pits.

At present time two dimensional steady aerodynamic model and pollution transport was developed by *Nuterman and Starchenko* (*2003*, *2004, 2005*). Mathematical model of the problem includes Reynolds equations, which have been written with the use of Boussinesq closing assumption:

$$\frac{\partial U}{\partial x}+\frac{\partial V}{\partial y}=0$$

$$U\frac{\partial U}{\partial x}+V\frac{\partial U}{\partial y}=-\frac{1}{\rho}\frac{\partial \widetilde{P}}{\partial x}+2\frac{\partial}{\partial x}\left[(\nu+\nu_T)\frac{\partial U}{\partial x}\right]+\frac{\partial}{\partial y}\left[(\nu+\nu_T)\frac{\partial U}{\partial y}\right]+\frac{\partial}{\partial y}\left[(\nu+\nu_T)\frac{\partial V}{\partial x}\right]-F_x,$$

$$U\frac{\partial V}{\partial x}+V\frac{\partial V}{\partial y}=-\frac{1}{\rho}\frac{\partial \widetilde{P}}{\partial y}+\frac{\partial}{\partial x}\left[(\nu+\nu_T)\frac{\partial V}{\partial x}\right]+2\frac{\partial}{\partial y}\left[(\nu+\nu_T)\frac{\partial V}{\partial y}\right]+\frac{\partial}{\partial x}\left[(\nu+\nu_T)\frac{\partial U}{\partial y}\right]-F_y.$$

Here U,V - is projections of velocity vector to axes Ox and Oy, ν - kinematic viscosity of air; ν_T - turbulent viscosity; $\widetilde{P}=P+\frac{2}{3}\rho k$, where P - pressure, k - kinetic energy of turbulence, ρ - density, F_x,F_y - projection of resistance force of air motion in vegetation canopy. The expressions for F_x,F_y are $F_x=\eta C_f aU\sqrt{U^2+V^2}$, $F_y=\eta C_f aV\sqrt{U^2+V^2}$, where η - part of surface, covered by trees, C_f - resistance factor, a - density of vegetation in forested canopy (for instance, for pine trees $\eta=1$, C_f =0.2, a =0.3125 m^2/m^3 (*Kimura et al., 2003*).

The boundary conditions for the system of Reynolds equations are as follows:

- on the left boundary at $x = 0$: $U(0,y)=U_{300}\left(\frac{y-Ly_1}{300-Ly_1}\right)^{0.3}$;

$$V(0,y)=0.$$

- on the right boundary at $x = Lx$ simple boundary conditions of stream stabilization are used:

$$\frac{\partial U}{\partial x}=\frac{\partial V}{\partial x}=0.$$

- on the walls non-slip conditions are used: $U=V=0$.
- on the top boundary it is assumed that velocity components are known:

$$U=U_{300}\left(\frac{Ly-Ly_1}{300-Ly_1}\right)^{0.3};$$

$$V=0.$$

To define turbulent parameters of a flow the modified (*Leschziner and Rodi, 1984*) k-ε model of turbulence (*Launder and Spalding, 1974*) is used:

$$U\frac{\partial k}{\partial x}+V\frac{\partial k}{\partial y}=\frac{\partial}{\partial x}\left[\left(\nu+\frac{\nu_T}{\sigma_k}\right)\frac{\partial k}{\partial x}\right]+\frac{\partial}{\partial y}\left[\left(\nu+\frac{\nu_T}{\sigma_k}\right)\frac{\partial k}{\partial y}\right]+G-\varepsilon+F_k;$$

$$U\frac{\partial \varepsilon}{\partial x}+V\frac{\partial \varepsilon}{\partial y}=\frac{\partial}{\partial x}\left[\left(\nu+\frac{\nu_T}{\sigma_\varepsilon}\right)\frac{\partial \varepsilon}{\partial x}\right]+\frac{\partial}{\partial y}\left[\left(\nu+\frac{\nu_T}{\sigma_\varepsilon}\right)\frac{\partial \varepsilon}{\partial y}\right]+(c_1G-c_2\varepsilon)\frac{\varepsilon}{k}+F_\varepsilon;$$

$$\nu_T=c_\mu\frac{k^2}{\varepsilon},\qquad(4.1)$$

where ε - dissipation of turbulent energy k, production of energy turbulence $G=\nu_T\left[2\left(\frac{\partial U}{\partial x}\right)^2+2\left(\frac{\partial V}{\partial y}\right)^2+\left(\frac{\partial U}{\partial y}+\frac{\partial V}{\partial x}\right)^2\right]$, constants $c_1=1.44$, $c_2=1.92$, $\sigma_k=1.0$, $\sigma_\varepsilon=1.3$, F_k,F_ε - additional source terms, modeling the influence of vegetation on turbulence : $F_k=U\cdot F_x+V\cdot F_y$, $F_\varepsilon=\frac{\varepsilon}{k}C_{p\varepsilon 1}(U\cdot F_x+V\cdot F)$ where $C_{p\varepsilon 1}=2.0$ (*Kimura et al., 2003*).

Moving vehicles are not only sources of pollutant emissions into the atmosphere, but also generators of the so-called mechanical turbulence, caused by the air disturbance as a result of motion of a finite-length objects having a significant resistance. In this work, this factor is taken into account as

in (*Louka,* 2003) by adding the corresponding terms into the *k*-ε model of turbulence. The results of calculations have shown that the addition of the mechanical turbulence to the model leads to increase of the role of the turbulent diffusion in the pollutant spreading under urban conditions due to the increased level of turbulence. To take into account the generation of the kinetic energy of turbulence due to the traffic, the right-hand side of *k*-equation is complemented with the term $C_{car}V_{car}^2Q_{car}$ while ε-equation is complemented with the term responsible for the dissipation of the mechanical energy of turbulence, which has the form $C_{car}V_{car}^2Q_{car}\frac{\varepsilon}{k}$ where C_{car} = 0.0015 is the empirical coefficient; V_{car} is the vehicle speed; Q_{car} is the number of vehicles per second (*Louka*, 2003).

In this work, we consider two versions of the closure relation Eq. (4.1). In the first case, the coefficient c_μ is equal to 0.09, as in the original *k*-ε model (*Launder and Spalding, 1974*). In the second case, the influence of the curvature of flow lines on the turbulent stress tangents and on the degree of anisotropy of normal stresses is taken into account (*Leschziner and Rodi, 1984*):

$$c_\mu = \frac{0.09}{\left[1+0.285\frac{k^2}{\varepsilon^2}\cdot\frac{\partial U_s}{\partial n}\cdot U_{ss}\cdot\Omega\right]}, \qquad (4.2)$$

where $\frac{\partial U_s}{\partial n} = U_{ss}\cdot\Omega+\Omega_1\sin(2\theta)+(\Omega_2+\Omega_3)\cos(2\theta)$,

with $\Omega = (\Omega_1\cdot U\cdot V+\Omega_2U^2-\Omega_3V^2)/U_{ss}^3$, $\Omega_1=\frac{\partial V}{\partial y}-\frac{\partial U}{\partial x}$, $\Omega_2=\frac{\partial V}{\partial x}$, $\Omega_3=\frac{\partial U}{\partial y}$,

$\theta = arctg\left(\frac{U}{V}\right)$, $U_{ss}=\sqrt{U^2+V^2}$.

Boundary conditions for two-equation model are the following:

- on the left boundary at $x = 0$: $k = k_0(y), \varepsilon = \varepsilon_0(y)$;
- on the right boundary at $x = Lx$: $\frac{\partial k}{\partial x}=\frac{\partial \varepsilon}{\partial x}=0$;
- on the upper boundary at $y = Ly$: $\frac{\partial k}{\partial y}=\frac{\partial \varepsilon}{\partial y}=0$.

For the definition of values of parameters near to the wall the Launder-Spalding method of the near-wall functions is used (*Launder and Spalding, 1974*).

The field of concentration of polluting substance is determined from the solution of the equation of impurity transport:

$$\frac{\partial(UC)}{\partial x}+\frac{\partial(VC)}{\partial y}=\frac{\partial}{\partial x}\left[\left(\frac{\nu}{Sc}+\frac{\nu_T}{Sc_T}\right)\frac{\partial C}{\partial x}\right]+\frac{\partial}{\partial y}\left[\left(\frac{\nu}{Sc}+\frac{\nu_T}{Sc_T}\right)\frac{\partial C}{\partial y}\right]+I.$$

This differential equation integrated with zero boundary condition for pollutant concentration on the left boundary and simple gradient conditions on other boundaries. The problem is solved numerically. Discretization of the differential equations is carried out by the finite volume method (*Patankar*, *1980*). For verification of model and method of solving the set of tests was carried out.

Test 1. Turbulent motion behind a ledge (*Durst et al., 1979*).

The ledge height is *h* = 0.076 m, and the fluid velocity in the entrance cross section is 10 m/s. The flow pattern corresponds to the Reynolds number of 50 000. The calculations were carried out in a region with the dimensions of 2 m along the axis *Ox* and 0.4 m along the axis *Oy* on a 150×80 grid

at $c_\mu = 0.09$ and with allowance for influence of the flow line curvature on the turbulent structure of the flow c_μ is calculated by Eq. (4.2).

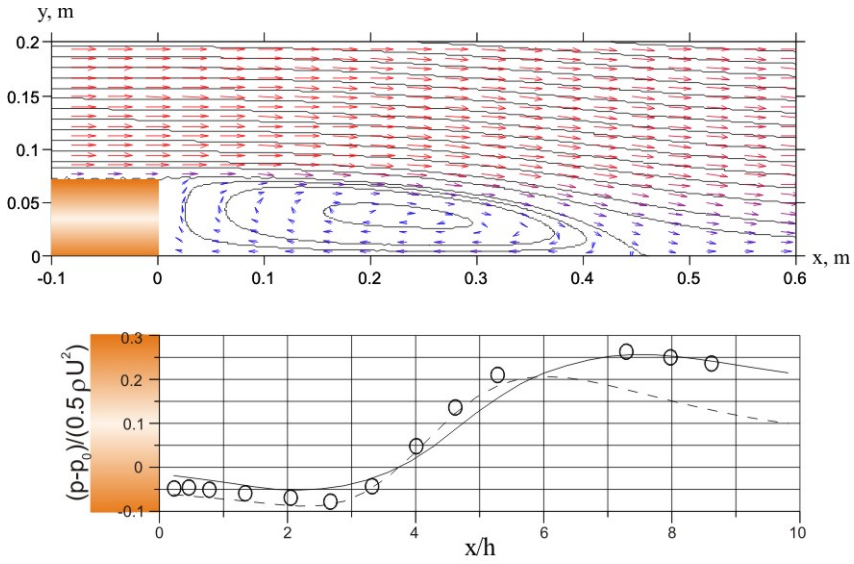

Figure 4.1: Vector field and current streamlines and distribution of the pressure coefficient behind a reward-facing ledge: --- $c_\mu = 0.09$, — c_μ is calculated by Eq. (4.2), o - experiment (*Durst et al., 1979*).

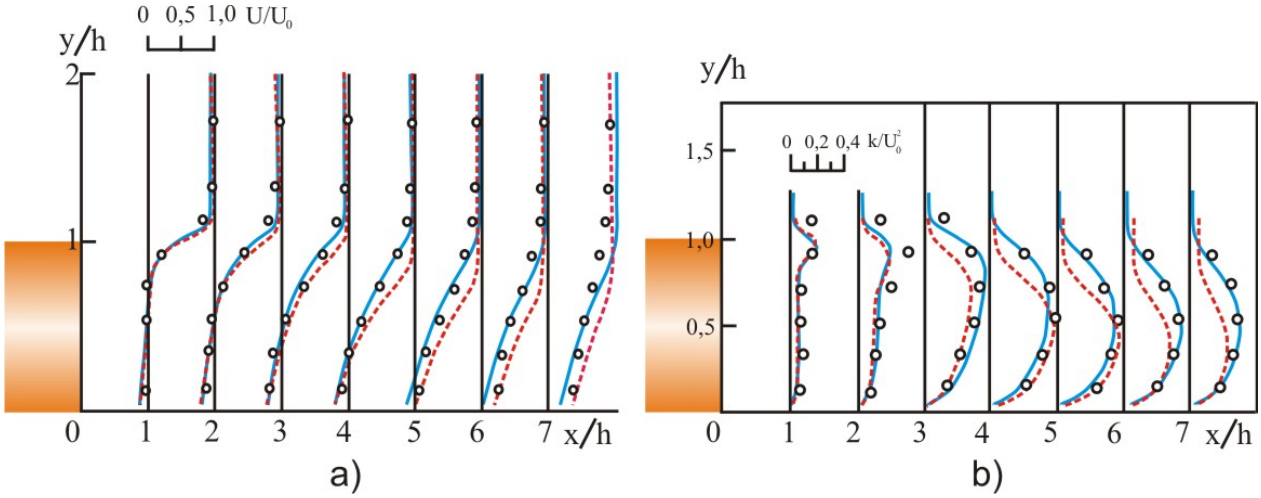

Figure 4.2: Profiles of velocity (a) and the kinetic energy of turbulence (b) behind a ledge; --- $c_\mu = 0.09$, ···· c_μ is calculated by Eq. (4.2), o - experiment (*Durst et al., 1979*).

Figures 4.1 and 4.2 show the vector field of the turbulent motion behind the ledge, the plot of variation of the pressure coefficient, the dimensionless velocity, and the kinetic energy of the turbulence downstream.

Calculations show that, when using the standard k-ε model, the recirculation flow zone is smaller than it actually is. The modification of the turbulence model in order to take into account the influence of the flow line curvature on the turbulent structure allows more accurate calculation of the recirculation zone.

Test 2. Pollutant transport in a street canyon.

The dimensionless concentration of a pollutant in the street canyon was calculated as a function of the wind direction, and the results obtained were compared with other similar model results and with experimental data from (*Ketzel et al., 2000*). The dimensionless concentration was determined as $c^* = C \cdot U_{Href} \cdot H / I$, where C is the concentration at the left wall of the canyon; U_{Href} is the velocity at the height H_{ref} (for example, 100 m); H is the characteristic height (for example, mean height of buildings, equal to about 16 m), and I is the intensity of the source of pollution. The results were compared with those obtained by the following models: MISKAM 1.1 (2D Microscale Flow and Dispersion Model), MISKAM 3.51, MISKAM 3.6 (3D Microscale Flow and Dispersion Models) (*Eichhorn, 1998*), and OSPM (Danish 2D Operational Street Pollution Model) (*Berkowicz et al., 1997*). Figure 4.3 shows the results obtained for the canyon of an ideal shape with the width and height of 16 m and the length of 90 m. By the symmetry reasons, the results are shown only for directions from 90° to 270°; the direction of 180° corresponds to the flow parallel to the street.

The best agreement with the results in a wind tunnel (*Ketzel et al., 2000*) was obtained for the MISKAM 1.1 model. The latest versions of this model predict both the overestimated concentrations in the windward side (90°, MISKAM. 3.51) and underestimated ones (in comparison with the experiment) on the leeward side (270°, MISKAM. 3.6). OSPM gives larger values, except for the direction of 270°, where the clearly pronounced maximum is not achieved. Analogous calculations by developed model (the result is shown in Fig. 4.4) clearly demonstrate that the concentration level is low on the windward side. It should be noted that, in general, the agreement with the experimental data from (*Ketzel et al., 2000*) is good.

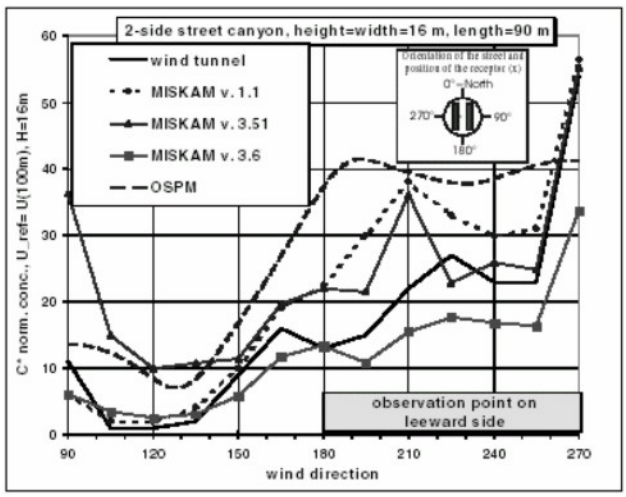

a)

Figure 4.3: Dimensionless concentration in a street canyon as a function of the wind direction (*Ketzel et. al., 2000*).

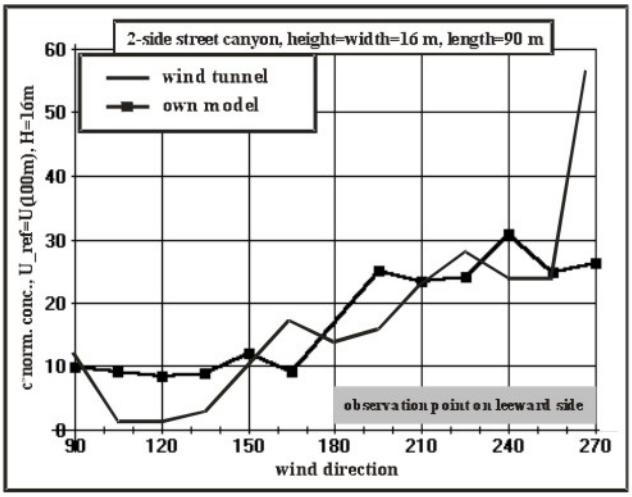

b)

Figure 4.4: Dimensionless concentration in a street canyon as a function of the wind direction (calculations by the developed model).

Summarizing the results of above calculations, comparison with experimental data and also with similar models one could say that suggested model satisfactory predicts the air flow in areas with complex geometry and pollution dispersion in urban canopy. Therefore it will be apply for air flow modeling in urban street canyon and air pollution from traffic.

The proposed mathematical model was applied to the study of flow aerodynamics and the transport of a traffic pollutant in urban building elements. The calculations were carried out on a 161×121

grid. The pollution sources of constant intensity were located near the surface ($y = 0.5$ m). The velocity of the incoming flow was U_{300} = 1 m/s. In the calculations, we took the traffic speed $V_{car} = 10$ m/s, and the traffic intensity $Q_{car} = 0.5$ s^{-1}. The location of pollution sources coincides with mechanical turbulence sources. The following cases were considered:

Table 1.

Case number	Width	Height	Wind speed	Comments
1	W = 20 m	H = 20 m	U_{300} = 1 m/s	the source of pollution and mechanical turbulence in point (x = 45 m, y = 0.5 m); W, H – width and height of street canyon; (Figure 4.5 a)
2	W = 20 m	H = 20 m	U_{300} = 1 m/s	the source of pollution and mechanical turbulence in point (x = 37 m, y = 0.5 m); (Figure 4.5 b)
3	W = 20 m	H = 20 m	U_{300} = 1 m/s	the source of pollution and mechanical turbulence in point (x = 37 m, y = 0.5 m); (the vegetation area is 42,5 m≤ x ≤47,5 m; 1 m≤ y ≤10 m); (Figure 4.5 c)
4	W = 20 m	H = 5 m	U_{300} = 1 m/s	the source of pollution and mechanical turbulence in point (x = 45 m, y = 0.5 m); (Figure 4.6 a)
5	W = 40 m	H = 5 m	U_{300} = 1 m/s	the source of pollution and mechanical turbulence in point (x = 45 m, y = 0.5 m); (Figure 4.6 b)
6	W = 40 m	H = 5 m	U_{300} = 1 m/s	the source of pollution and mechanical turbulence in point (x = 37 m, y = 0.5 m); (Figure 4.6 c)
7	W = 40 m	H = 5 m	U_{300} = 1 m/s	the source of pollution and mechanical turbulence in point (x = 37 m, y = 0.5 m); (Figure 4.6 d); (the vegetation area is 40 m ≤ x ≤ 50 m; 1 m ≤ y ≤ 10 m)

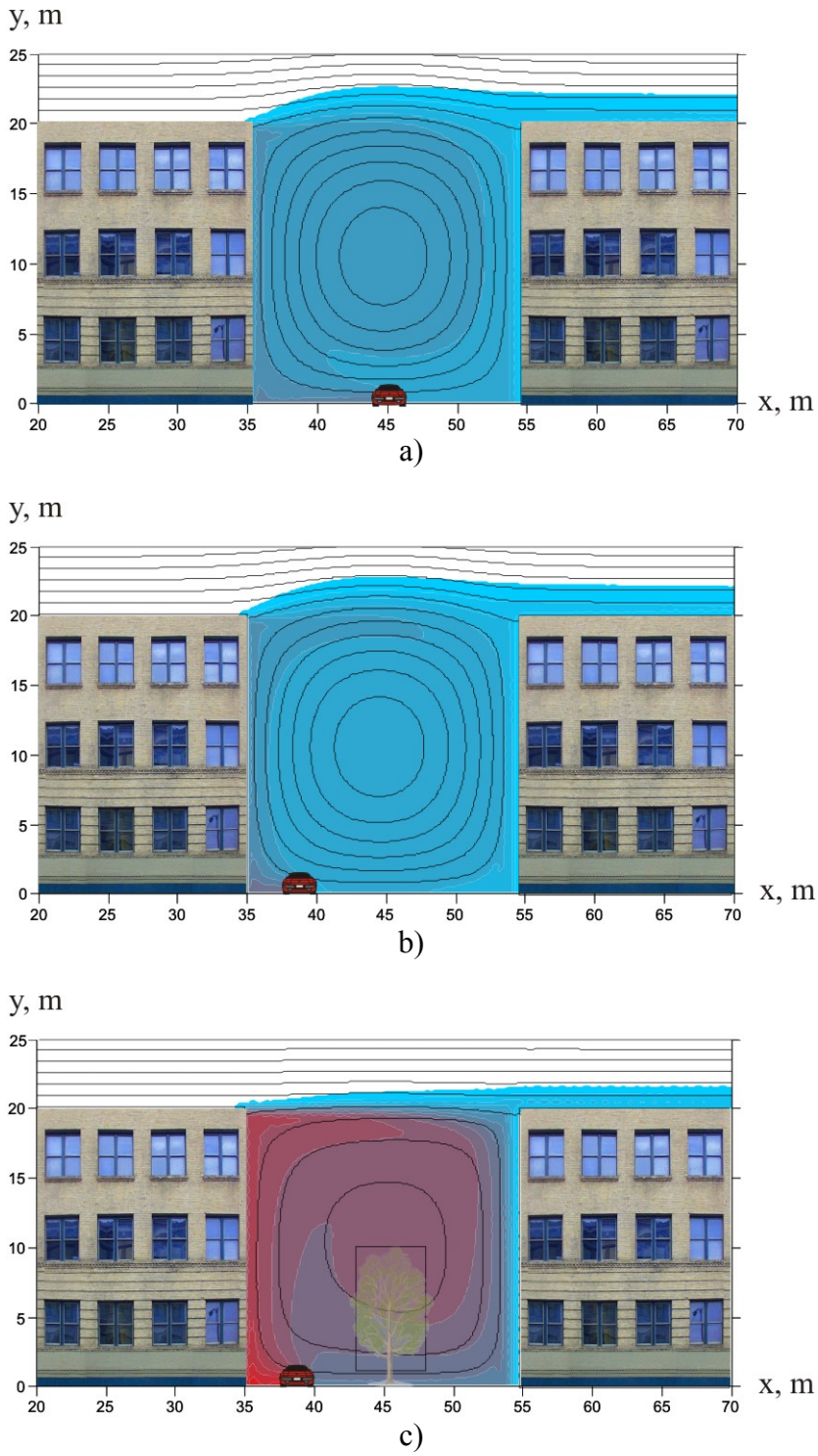

Figure 4.5: Streamlines and distribution of the pollutant concentration in the street canyon with $W = 20$ m; $H = 20$ m; the vegetation area is shown by a rectangle; a) the source of pollution at (x = 45 m, y = 0.5 m); b), c) the pollution source at (x = 37 m, y = 0.5 m).

The results calculated indicate that the circulating motion of air is formed in the canyon; and the motion direction and intensity are determined by the main flow velocity Figures 4.5 (a), (b), (c). The pollutant, emitted by sources located at the canyon bottom and entrained by the circulating motion of air, is transported to the leeward side, and then it is partly carried into the main flow and partly returned into the region bounded by the vertical walls of neighboring buildings. The recirculation flow speed in the canyon is much lower that the air speed above buildings, which favors the formation of the increased level of the pollutant concentration all over the canyon volume and,

especially, near the emission sources and near the leeward side of the canyon. It should be noted that the change in the street canyon volume influences the level of air pollution in it, but local maximal values of pollutant concentrations are always observed near the leeward side of the canyon.

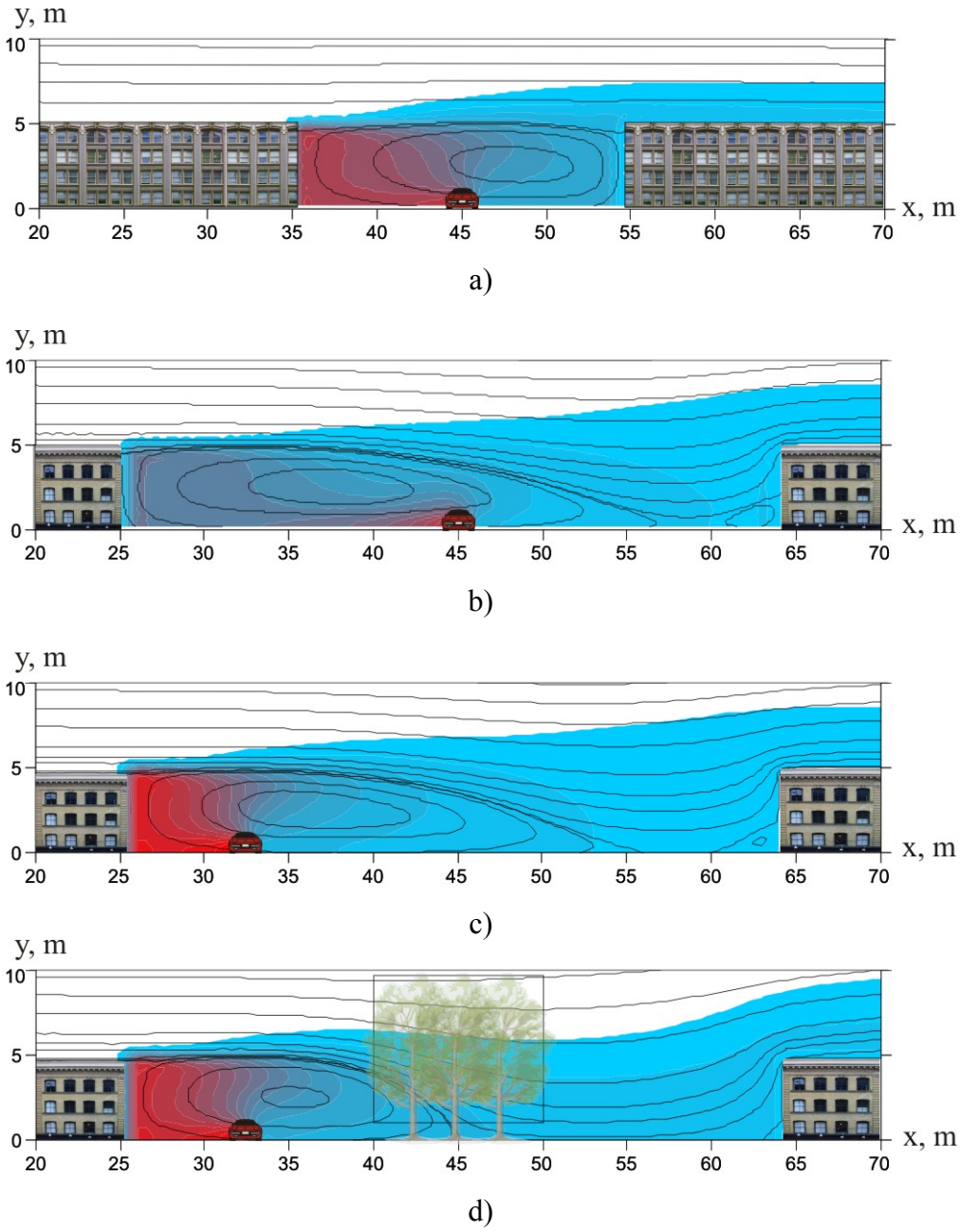

Figure 4.6: Streamlines and distribution of the pollutant concentration in the street canyon; the vegetation area is shown by a rectangle; a) $W = 20$ m; $H = 5$ m, the of pollution source at (x = 45 m, y = 0.5 m); b) $W = 40$ m; $H = 5$ m, the pollution source at (x = 45 m, y = 0.5 m); c) $W = 40$ m; $H = 5$ m, the pollution source at (x = 37 m, y = 0.5 m); d) $W = 40$ m; $H = 5$ m, the pollution source at (x = 37 m, y = 0.5 m);

A small vegetation area (few pine trees) at the center of the street canyon (Figures 4.5 (a), 4.6 (d)), all other parameters of calculation being the same, significantly decreases the speed of the circulating motion due to the increased resistance to the flow. In addition, the appearance of a penetrable obstacle in the street canyon leads to deformation of current streamlets in the vegetation zone and behind it due to lifting motion of air having passed near the obstacle bottom. The intensity of the street canyon ventilation decreases, leading to increase in the level of the pollutant concentration all

over the canyon volume and, especially, near the leeward side. The intensification of the turbulent transport caused by a change in the character of the recirculating motion, which shows itself as a lifting turbulized polluted flow behind a penetrable obstacle, favors the additional dispersion of the pollutant.

It is also important to note that geometrical parameters of street canyon have significant influence on flow pattern and concentration of pollution. Ratio $H/W = 0.25$ (Figure 4.6 (a)) is described by vortex stretching along street canyon, and it displacement to windward building, that result in increasing of concentration level at lee side. Further increasing of distance between two buildings ($H/W = 0.125$) result in formation of two recirculating zones: big vortex at leeward building and small vortex at windward side (Figures 4.6 (b), (c)). In this case the impurity, induced from traffic, which located at the center of canyon, removed to leeward building, recirculating and amass there.

This two-dimensional mathematical model is the beginning stage of developing tree-dimensional non-steady micro-scale model of atmosphere aerodynamics and pollution transport in urban canopy. In the future the implementation of chemistry, insolation effects, thermal budget and deposition, which can influence on air flow structure and impurity transport, especially in stagnation regions, will be realized in the model. Moreover, the downscaling/integration of the obstacle-resolved micro-scale model with a city-scale model, such as DMI-Enviro-HIRLAM, is suggested and an interface part for models interaction using the nesting technology will be realized.

Conclusions

The review of literature concerning turbulence closure and approaches of pollution dispersion and heat transfer modeling was made. The basic advantages and disadvantages of different types of turbulence models were presented.

On the basis of existing knowledge and modeling experience a mathematical numerical model for investigation of aerodynamics in urban building elements was constructed. The model was tested in 2D version and demonstrated a good agreement with the experimental data and others similar models.

The distribution of the concentration of a gaseous pollutant emitted by continuous sources, such as traffic, has been calculated in the street canyon and near some isolated building. The basic three types of airflow in urban street canyons were modeled. The results of simulations show that the increasing of canyon volume leads to decreasing of concentrations. Moreover, the geometrical characteristics influence (high H and width W) on the flow pattern and can be cause of recirculation eddy stretching ($H/W = 0.25$) and formation of secondary vortex ($H/W = 0.125$).

The influence of a vegetation area located near the urban roadway and traffic induced turbulence on the aerodynamic pattern of the flow and the pollutant dispersion has been investigated. Such important factor as urban vegetation decreases the speed of the circulating motion and ventilation since the resistance to the flow increase, and its leads to rising of pollution levels. Besides, the traffic induced turbulence promotes more intensive mixing processes in urban street canyon.

This model is the first stage of developing tree-dimensional non-steady micro-scale model of atmosphere aerodynamics and pollution transport in urban canopy. On further stages the model will be improved using new turbulence closure schemes, incorporating chemistry, effects of insolation, thermal budget, deposition, etc. Moreover, the downscaling/integration of the obstacle-resolved micro-scale model with a city-scale model, such as DMI-Enviro-HIRLAM, using the nesting technology will be realized.

Acknowledgments

The authors wish to express their appreciation for support from the Danish Meteorological Institute (DMI). The funding of this study has been provided by two Young Scientist Grants: (i) from the Russian Federal Agency of Science and Innovations (N 02.444.11.7196) and (ii) from the INTAS: PhD fellowship "*Turbulent flow and transport modeling in urban canopy*" (Grant 06-1000016-5928), and by the EC 6FP project ENVIRO-RISKS (INCO-CT-2005-013427). The authors wish to acknowledge Alexander Mahura (DMI) for useful discussions and comments to the report.

References

Amosov, P. and A. Baklanov, 1992: Room ventilation on the base of numerical modelling of air- and thermodynamics, in *ROOMVENT'92*, Int. Conference, Aalborg, Denmark, Sept. 2-4, 1992, **1**, 273–288.

Baklanov, A. A., 2000: Application of CFD methods for modeling in air pollution problems: possibilities and gaps, *Environmental Monitoring and Assessment*, **65**, 181–189.

Baklanov, A., 1988: Numerical modeling in mine aerodynamics, Apatity: KSC, Russian Academy of Sciences, 200 p. (in Russian)

Baklanov, A., 2006: Overview of the European project FUMAPEX, *Atmos. Chem. Phys.*, **6**, 2005–2015.

Baklanov, A., and O. Hänninen, and L. H. Slørdal, and J. Kukkonen, and J. H. Sørensen, and N. Bjergene, and B. Fay, and S. Finardi, and S. C. Hoe, and M. Jantunen, and A. Karppinen, and A. Rasmussen, and A. Skouloudis, and R. S. Sokhi, 2006: Integrated systems for forecasting urban meteorology, air pollution and population exposure, *Atmos. Chem. Phys*., **7**, 855–874.

Baklanov, A., and A. Rasmussen, and B. Fay, and E. Berge, and S. Finardi, 2002: Potential and shortcomings of numerical weather prediction models in providing meteorological data for urban air pollution forecasting, *Water, Air and Soil Poll.: Focus*, **2**, 43–60.

Balaras, E., and C. Benocci, and U. Piomelli, 1995: Finite-difference computations of high Reynolds number flows using the dynamic subgrid-scale model, *Theoret. Comput. Fluid Dynamics*, **7**, 207–216.

Bardina, J., and J. H. Ferziger, and W. C. Reynolds, 1980: Improved subgrid-scale models for large eddy simulation, *AIAA J.*, **80,** 1357.

Baumer, D., and B. Vogel, and F. Fiedler, 2005: A new parameterisation of motorway-induced turbulence and its application in a numerical model, *Atmospheric Environment*, **39**, 5750–5759.

Berkowicz, R., and O. Hertel, and S. E. Larsen, and N. N. Sörensen, and M. Nielsen, 1997: Modelling traffic pollution in streets, *Report*, National Environment Research Institute, Roskilde, Denmark, 55 pp.

Brown, M. J., and R. E. Lawson, and D. S. DeCroix, and R. L. Lee, 2000: Mean flow and turbulence measurements around a 2-D array of buildings in a wind tunnel, *Proceedings of 11th Joint AMS/AWCMoAn f. on the Appl. of Air Poll. Met.*, Long Beach, CA., 35–40.

Chang, J. C., and S. R. Hanna, and Z. Boybeyi, and P. Franzese, 2004: Use of Salt Lake City Urban

2000 field data to evaluate the Urban HPAC dispersion model, *Journal of Applied Meteorology*, **44**, 485–501.

Cheng, Y., and F. S. Lien, and E. R. Yee, and R. Sinclair, 2003: A comparison of large eddy simulations with a standard k-ε Reynolds-averaged Navier-Stokes model for the prediction of a fully developed turbulent over a matrix of cubes, *Journal of Wind Engineering and Industrial Aerodynamics*, **91**, 1301–1328.

Chun-Ho, L., and M. C. Barton, and D. Y. C. Leung, 2004: Large-Eddy Simulation of Flow and Pollutant Transport in Street Canyons of Different Building-Height-to-Street-Width Ratios, *Journal of Applied Meteorology*, **43**, 1410–1424.

Colman, V., 1984: Methods of turbulent flows computation, *Mir*, Moscow, 464 pp.

COST715, 2003: COST Action 715: Workshop on urban boundary layer parameterisations. Eds. M. Rotach, and B. Fisher, and M. Piringer. EUR 20355, OOP EC, Luxembourg.

Craft, T. J., and B. E. Launder, and K. Suga, 1996: Development and application of a cubic eddy-viscosity model of turbulence, *Int. J. Heat and Fluid Flow*, **17**, 108–115.

Dumuren, A. O., 1991: Calculation of turbulent-driven secondary motion in ducts with arbitrary cross section, *AIAA J.*, **29**, N. 4, 531–537.

Durst, F., and B. E. Launder, and F. W. Schmidt, and J. H. Whitelaw, 1979: Turbulent shear flow I, *Springer-Verlag*, Berlin, 432 pp.

Dwyer, M. J., and E. G. Patton, and R. H. Shaw, 1997: Turbulent kinetic energy budgets from a large eddy simulation of airflow above and within a forest canopy, *Boundary-Layer Meteorology*, **84**, 23–43.

Ehrhard, J., and N. Moussiopoulus, 2000: On a new nonlinear turbulence model for simulating flows around building-shaped structures, *Journal of Wind Engineering and Industrial Aerodynamics*, **88**, 91–99.

Eichhorn, J., 1998: MISKAM-Handbuch zur Version 3.xx, Giese-Eichhorn, Wachernheim, Germany.

Gatski, T. B., and T. Jongen, 2000: Nonlinear eddy viscosity and algebraic stress models for solving complex turbulent flows, *Progress in Aerospace Science*, **36**, 655–682.

Gerdes, F., and D. Olivari, 2000: Analysis of pollutant dispersion in an urban street canyon, *Preprint institute Von Karman*, 21 pp.

Germano, M., and U. Piomelli, and P. Moin, and W. H. Cabot, 1991: A dynamic subgrid-scale eddy viscosity model, *Phys. Fluids,* **3A**, 1760–1765.

Hall, R. C., 1997: Evaluation of modeling uncertainty - CFD modeling of near field atmospheric dispersion. EU Project EV5V-CT94-0531, *Final Report.* WS Atkins Consultants Ltd., Woodcote Grove, Ashley Road, Epsom, Surrey KT18 5BW, UK.

Huang, H., and Y. Akutsu, and M. Arai, and M. Tamura, 2000: A two-dimensional air quality model in an urban street canyon: evaluation and sensitivity analysis, *Atmospheric Environment*, **34**, 689–698.

Jordan, S. A., 2001: Dynamic subgrid-scale modeling for large-eddy simulations in complex topologies, *J. Fluids Engng.*, **123**, 619–627.

Katolicky, J., and M. Jicha, 2005: Eulerian-Lagrangian model for traffic dynamics and its impact on operational ventilation of road tunnels, *Journal of Wind Engineering and Industrial Aerodynamics*, **93**, 61–77.

Katul, G. G., and J. D. Albertson, 1998: An investigation of high-order closure models for a forested canopy, *Boundary-Layer Meteorology*, **89**, 47–74.

Ketzel, M., and R. Berkowiez, and A. Lohmeyer, 2000: Comparison of numerical street dispersion models with results from wind tunnel and field measurements, *Environmental Monitoring and Assessment*, **65**, 363–370.

Ketzel, M., and P. Louka, and P. Sahm, and E. Guilloteau, and J. F. Sini, and N. Moussiopoulos, 2001: Inter-Comparison of Numerical Urban Dispersion Models, *Proceedings, 3rd Int. Conf. on Urban Air Quality*, Loutraki, Greece.

Kimura, A., and T. Iwata, and A. Mochida, and H. Yoshino, and R. Ooka, and S. Yoshida, 2003: Optimization of Plant Canopy Model for Reproducing Aerodynamic Effects of Trees: (Part 1) Comparison between the canopy model optimized by the present authors and that proposed by Green, *Summaries of Technical Papers of Annual Meeting Architectural Institute of Japan*, **9**, 721–722.

Kolmogorov, A. N., 1942: Equations of turbulent motion of an incompressible fluid, *Izvestia Academy of Sciences*, USSR, Physics, **6**, N.1, 56–58.

Kurbatskii, A. F., and S. N. Yakovenko, 2000: Turbulence closure schemes suitable for air pollution and wind engineering, *Journal of Wind Engineering and Industrial Aerodynamics*, **87**, 231–241.

Launder, B. E, and D. B. Spalding, 1974: The numerical computation of turbulent flows, *Computational Methods in Applied Mechanics and Engineering*, **3**, N. 2, 269–289.

Launder, B. E., 1978: Heat and mass transfer, in: P. Bradshaw (Ed.), Topics in Physics, **12**, *Turbulence,* Springer, New York, 231–287.

Launder, B. E., and B. Spalding, 1972: Mathematical Models of Turbulence, *New York: Academic Press*.

Launder, B. E., and G. J. Reece, and W. Rodi, 1975: Progress in the development of Reynolds stress turbulent closure, *J. Fl. Mech.*, **68**, 537–566.

Leschziner, M. A., and W. Rodi, 1984: Computational of strongly swirling axisymmetric free jets, *AIAA J.*, **22**, N. 12, 1742–1747.

Lien, F. S., and W. L. Chen, and M. A. Leschziner, 1996: Low-Reynolds-number eddy-viscosity modeling based on non-linear stress- strain/vorticity relations, in: W. Rodi (Ed.), *Engineering Turbulence Modeling and Experiments 3*, Crete, Greece.

Lilly, D. K., 1966: On the application of the eddy viscosity concept in the inertial subrange of turbulence, NCAR-123, National Center for Atmospheric Research, Boulder, CO.

Lilly, D. K., 1992: A proposed modification of the Germano subgrid-scale closure methods, *Phys. Fluids*, **4A**, 633–635.

Louka, P., 2003: Contribution of Petroula Louka to the TRAPOS WG-TPT meeting in Cambridge, URL: http://www2.dmu.dk/atmosphericenvironment/Trapos/texte/louka-camb.pdf

Louka, P., and M. Ketzel, and P. Sahm, and E. Guilloteau, and N. Moussiopoulos, and J.-F. Sini, and P. G. Mestayer, and R. Berkowiez, 2001: CFD intercomparison exercise within TRAPOS European research network, *7th International Conference on Environmental Science and Technology*, **9**, 8 pp.

Mestayer, P. G., and J.-F. Sini, and M. Jobert, 1995: Simulation of the Wall Temperature Influence on Flows and Dispersion within Street Canyons, in Air Pollution '95, **1**, *Turbulence and Diffusion*, Porto Carras, Greece, September, 109–106.

Moin, P., and K. Squires, and W. Cabot, and S. Lee, 1991: A dynamic subgrid-scale model for compressible turbulence and scalar transport, *Phys. Fluids*, **3A**, N. 11, 2746–2757.

Neophytou, M. K., and R. E. Britter, 2004: A simple correlation for pollution dispersion prediction in urban areas, *DAPPLE Cambridge Note 1*, http://www.dapple.org.uk

Nisizima, S., and A. Yoshizawa, 1987: Turbulent channel and Couette flows using anisotropic k-ε turbulence model, *AIAA J.*, **25**, 414–420.

Nuterman, R. B., and A.V. Starchenko, 2003: Numerical simulation of airflows in a street canyon, *Atmos. Oceanic Opt.*, **16**, N. 5-6, 483–486.

Nuterman, R. B., and A.V. Starchenko, 2004: A modeling of air flow in a street canyon, *Proceedings of SPIE.*, **5396**, 89–98.

Nuterman, R. B., and A.V. Starchenko, 2005: Modeling of air pollution transport in urban street canyon, *Atmos. Oceanic. Opt.*, **18**, N. 8, 581–588.

Oke, T. R., 1988: Boundary Layer Climate, *Routledge*, London, 464 pp.

Patankar, S. V., 1980: Numerical Heat Transfer and Fluid Flow, *Hemisphere Pub. Corp.*, New York, 197 pp.

Piomelli, U., 1993: High Reynolds number calculations using the dynamic subgrid-scale stress model, *Phys. Fluids*, **5A**, N. 6, 1484–1490.

Pope, S., 1975: A more general effective-viscosity hypothesis, *J. Fluid Mech.*, **72**, 331–340.

Rodi, W., 1976: A new algebraic relation for calculating Reynolds stresses, *ZAMM*, **56**, 219–221.

Rodi, W., 1997: Comparison of LES and RANS calculations of the flow around bluff bodies, *Journal of Wind Engineering and Industrial Aerodynamics*, **69**, N. 71, 55–75.

Rotach, M. W., and S-.E. Gryning, and E. Batchvarova, and A. Christen, and R. Vogt, 2004: Pollutant dispersion close to an urban surface - the BUBBLE tracer experiment, *Metorol. Atm. Phys.*, **87**, N. 1-3, 39–56.

Rubinstein, R., and J. M. Barton, 1990: Non-linear Reynolds stress models and renormalization group, *Phys. Fluids*, **2A**, 1472–1476.

Schatzmann, M., and B. Leitl, 2002: Validation and application of obstacle resolving urban dispersion models, *Atmospheric Environment*, **36**, 4811–4821.

Shih, T. H., and J. Zhu, and J. L. Lumley, 1993: A realizable Reynolds stress algebraic equation models, *NASA tech. memo*, 105993.

Smagorinsky, J., 1963: General circulation experiments with the primitive equations, part I: The basic experiment, *Mort. Weather Rev.*, **91**, 99–164.

Speziale, C. G., 1987: On non-linear *k-l* and *k-ε* models of turbulence, *J. Fluid Mech.*, **178**, 459–457.

Walton, A., and A. Y. S. Cheng, and W. C. Yeung, 2002: Large-eddy simulation of pollution dispersion in an urban street canyon - Part I: comparison with field data, *Atmospheric Environment*, **36**, 3601–3613.

Wilcox, D. C., 1988: Multiscale model for turbulent Flows, *AIAA J.*, **26**, N. 11, 1311–1320.

Yang, K. S., and J. H. Ferziger, 1993: Large-eddy simulation of turbulent obstacle flow using a dynamic subgrid-scale model, *AIAA Journal*, **31**, 1406–1413.

Yoshzawa, A., 1986: Statistical theory for compressible turbulent shear flows with the application to subgrid modeling, *Phys. Fluids*, **29A**, 2152–2164.

Annex A. Averaging Approaches and Two-equation Models

Time averaging

For this approach, any variable f is assumed to be the sum of its mean quantity $\bar{f}$ and its fluctuation part f',

$$f(x,t) = \bar{f}(x,t) + f'(x,t),$$

where $\bar{f}$ is the time average of f,

$$\bar{f}(x,t) = \frac{1}{\Delta t}\int_{t}^{t+\Delta t} f(x,t)dt,$$

with

$$\overline{f'} = \frac{1}{\Delta t}\int_{t}^{t+\Delta t} f'dt = 0.$$

The time average of the product of fluctuation parts of two different variables f' и g' is given by:

$$\overline{f'g'} = \frac{1}{\Delta t}\int_{t}^{t+\Delta t} f'g'dt \neq 0.$$

Here, the time interval Δt is chosen compatible with the time scale of the turbulent fluctuations, not only for the variable f but also for other variables within the physical domain.

Ensemble averaging

In terms of measurements of N identical experiments, $f(x,t) = f_n(x,t)$, we may determine the average,

$$\bar{f}(x,t) = \lim_{N\to\infty} \frac{1}{N} \sum_{n=1}^{N} f_n(x,t) .$$

Volume averaging

When the flow variable is uniform on the average such as in homogeneous turbulence, we may choose to use a spatial average defined as

$$\bar{f}(t) = \lim_{\Omega\to 0} \frac{1}{\Omega} \int_{\Omega} f(x,t) d\Omega .$$

Favre averaging

For compressible flows, it is often more convenient to use mass (Favre) averages instead of time averages,

$$f = \tilde{f} + f'' ,$$

where the mean quantity is defined as

$$\tilde{f} = \frac{\overline{\rho f}}{\bar{\rho}} = \bar{f} + \frac{\overline{\rho' f'}}{\bar{\rho}} ,$$

and the fluctuation has the property $\overline{\rho f''} = 0$, whereas $\overline{f''} = -\overline{\rho' f'} / \bar{\rho} \neq 0$ for the case of a time average. It is clear that the correlation of density fluctuations, ρ', with the fluctuating quantity, f', gives rise to a nonzero mean Favre fluctuation field, $\overline{f''}$. Thus, it is seen that the Favre average makes the turbulent compressible flow equations simpler with their form resembling those of incompressible flows. Despite these simplifications, however, the density fluctuations or compressibility effects must still be resolved; only the mathematical simplifications are achieved through Favre averages.

The transport equations for k and ε may be written as follows:

$$\rho \frac{\partial k}{\partial t} + \rho \frac{\partial}{\partial x_i}(k\bar{v}_i) = \tau_{ij}^* \frac{\partial \bar{v}_j}{\partial x_i} - \rho\varepsilon + \frac{\partial}{\partial x_i}\left(\mu_k \frac{\partial k}{\partial x_i} \right),$$

$$\rho \frac{\partial \varepsilon}{\partial t} + \rho \frac{\partial}{\partial x_i}(\varepsilon\bar{v}_i) = c_{\varepsilon 1} \frac{\varepsilon}{k} \tau_{ij}^* \frac{\partial \bar{v}_j}{\partial x_i} - c_{\varepsilon 2} \rho \frac{\varepsilon^2}{k} + \frac{\partial}{\partial x_i}\left(\mu_\varepsilon \frac{\partial \varepsilon}{\partial x_i} \right),$$

with $\mu_k = \mu + \frac{\mu_T}{\sigma_k}$, $\mu_\varepsilon = \mu + \frac{\mu_T}{\sigma_\varepsilon}$, $c_\mu = 0.09$, $c_{\varepsilon 1} = 1.45 \sim 1.55$, $c_{\varepsilon 2} = 1.92 \sim 2.00$, $\sigma_k = 1$, $\sigma_\varepsilon = 1.3$.

Notice that the first, second, and third terms on the right-hand side of turbulence model correspond to the production, dissipation, and transport terms, respectively. The closure constants are obtained from the experimental data.

The transport equations for k and ω may be written as

$$\rho \frac{\partial k}{\partial t} + \rho \frac{\partial}{\partial x_i}(k\bar{v}_i) = \frac{\partial}{\partial x_i}\left((\mu + \sigma^* \mu_T) \frac{\partial k}{\partial x_i} \right) + \tau_{ij}^* \frac{\partial \bar{v}_j}{\partial x_i} - \beta^* \bar{\rho} k\omega ,$$

$$\rho \frac{\partial \omega}{\partial t} + \rho \frac{\partial}{\partial x_i}(\omega\bar{v}_i) = \frac{\partial}{\partial x_i}\left((\mu + \sigma\mu_T) \frac{\partial \omega}{\partial x_i} \right) + \alpha \frac{\omega}{k} \tau_{ij}^* \frac{\partial \bar{v}_j}{\partial x_i} - \beta\bar{\rho}\omega^2 ,$$

with the closure constants, $\alpha = 5/9$, $\beta = 3/40$, $\beta^* = 9/10$, $\sigma = 1/2$, $\sigma^* = 1/2$.

Annex B. Filters and Momentum Equations for Large Eddy Simulation

Filters for LES

Box

$$G(x) = \begin{cases} 1/\Delta, & if\ |x| \le \Delta/2 \\ 0, & otherwise \end{cases}$$

Gaussian

$$G(x) = \sqrt{\frac{6}{\pi\Delta^2}} \exp\left(-\frac{6x^2}{\Delta^2}\right),$$

Fourier cutoff

$$\hat{G}(k) = \begin{cases} 1, & if\ k \le \pi/2 \\ 0, & otherwise \end{cases}$$

The test filter operation can be performed as

$$\langle f(x,t)\rangle = \int \langle G(x,\xi)\rangle f(\xi,t) d\xi .$$

If the box function is used, we have

$$\langle G(x,\xi)\rangle = \begin{cases} 1/\Delta_t & if\ x_i - \Delta_t/2 \le \xi_i \le x_i + \Delta_t/2 \\ 0 & otherwise \end{cases}$$

The test filter can be calculated using the trapezoidal rule, Simpson's rule, or interpolation function methods.

After filtering the momentum equation takes the form

$$\frac{\partial \overline{v}_j}{\partial t} + \frac{\partial \left(\overline{v_i v_j}\right)}{\partial x_i} = -\frac{1}{\rho}\frac{\partial \overline{p}}{\partial x_j} + \frac{\partial \overline{\tau}_{ij}}{\partial x_i},$$

with

$$\begin{aligned} \overline{v_i v_j} &= \overline{(\overline{v}_i + v_i')(\overline{v}_j + v_j')} = \overline{\overline{v}_i \overline{v}_j} + \overline{v_i' \overline{v}_j} + \overline{\overline{v}_i v_j'} + \overline{v_i' v_j'} \\ &= \overline{\overline{v}_i \overline{v}_j} + \overline{v}_i \overline{v}_j - \overline{v}_i \overline{v}_j + \overline{v_i' \overline{v}_j} + \overline{\overline{v}_i v_j'} + \overline{v_i' v_j'} \\ &= \overline{v}_i \overline{v}_j - \tau_{ij}^* . \end{aligned} \qquad \text{(B.1)}$$

Substituting (B.1) into momentum equation yields

$$\frac{\partial \overline{v}_j}{\partial t} + \frac{\partial \left(\overline{v}_i \overline{v}_j\right)}{\partial x_i} = -\frac{1}{\rho}\frac{\partial \overline{p}}{\partial x_j} + \frac{\partial \overline{\tau}_{ij}}{\partial x_i} + \frac{\partial \tau_{ij}^*}{\partial x_i},$$

with the subgrid stress tensor τ_{ij}^* identified as

$$-\tau_{ij}^* = L_{ij} + C_{ij} + R_{ij} = \overline{v_i v_j} - \overline{v}_i \overline{v}_j ,$$

where L_{ij}, C_{ij} and R_{ij} are known as the Leonard stress tensor, cross stress tensor, and subgrid scale Reynolds stress tensor, respectively.

$$L_{ij} = \overline{\overline{v}_i \overline{v}_j} - \overline{v}_i \overline{v}_j ,$$

$$C_{ij} = \overline{v_i' \overline{v}_j} + \overline{\overline{v}_i v_j'} ,$$

$$R_{ij} = \overline{v_i' v_j'} \,.$$

Here, the Leonard stress represents the interaction between resolved scales, transferring energy to small scales (known as outscatter). The Leonard stress can be computed explicitly from the filtered velocity field. The cross stress represents the interaction between resolved and unresolved scales, transferring energy to either large or small scales. The subgrid scale Reynolds stress represents the interaction of two small scales, producing energy from small scales to large scales (known as backscatter).

The cross stress tensor may be simplified in terms of resolved scales using the so-called Galilean scale similarity model (*Bardina et al., 1980*).

$$C_{ij} = \overline{v_i' \overline{v}_j} + \overline{\overline{v}_i v_j'} = \overline{v}_i \overline{v}_j - \overline{\overline{v}_i \overline{v}_j} \,.$$

Summing stated above, yields:

$$L_{ij} + C_{ij} = \overline{\overline{v}_i \overline{v}_j} - \overline{\overline{v}_i \overline{v}_j} \,.$$

It is seen that the sum of the Leonard and cross stresses can be calculated from the resolved scales and thus only the subgrid scale Reynolds stress need be modeled. Thus, the turbulent stress tensor to be modeled as

$$-\tau_{ij}^{*} = \overline{v_i v_j} - \overline{v}_i \overline{v}_j \,.$$